Received: 27 September 2021 | Revised: 28 January 2022 | Accepted: 30 January 2022

DOI: 10.1002/jmor.21460

RESEARCH ARTICLE

Journal of morphology WILEY

Collagenic architecture and morphotraits in a marine basal metazoan as a model for bioinspired applied research

Renata Manconi[1] | Tiziana Cubeddu[1] | Roberto Pronzato[2] | Marina A. Sanna[1] | Gabriele Nieddu[3] | Elda Gaino[4] | Giacinta A. Stocchino[1]

[1]Dipartimento di Medicina Veterinaria, Università di Sassari, Sassari, Italy

[2]Dipartimento di Scienze della Terra, dell'Ambiente e della Vita, Università di Genova, Genoa, Italy

[3]Dipartimento di Scienze Biomediche, Università di Sassari, Sassari, Italy

[4]Viale Canepa 15/10, Genoa, Italy

Correspondence
Renata Manconi, Dipartimento di Medicina Veterinaria, Università di Sassari, Via Vienna 2, 07100 Sassari, Italy.
Email: renata.manconi@uniss.it

Funding information
This research was supported by Fondazione di Sardegna (FdS-2016 grant n. CUP J86C1800082005 "*La spongicoltura come fonte rinnovabile di prodotti bioattivi e biomimetici*"), Regione Autonoma Sardegna (RAS2012-L.R. 7/2007 grant no. CRP-60215) and Parco Nazionale dell'Asinara (PNA-2016). Giacinta A. Stocchino thanks both latter projects and Università di Genova for financial support. Other financial support was provided by *Università di Sassari-Fondo di Ateneo per la Ricerca* to Renata Manconi and Gabriele Nieddu (2019–2021). Gabriele Nieddu thanks "Programma Operativo Nazionale (PON) Ricerca e Innovazione 2014–2020—Asse I *Capitale Umano*, Azione I.2—A.I.M. Attraction and International Mobility, Linea 1 Mobilità dei ricercatori, AIM1874325-3, CUP J54I18000110001" and Fondazione di Sardegna (FdS-2016 grant CUP J86C1800082005) for financial support.

Abstract

In some Porifera (Demospongiae: Keratosa), prototypes of the connective system are almost exclusively based on collagenic networks. We studied the topographic distribution, spatial layout, microtraits, and/or morphogenesis of these collagenic structures in *Ircinia retidermata* (Dictyoceratida: Irciniidae). Analyses were carried out on a clonal strain from sustainable experimental mariculture by using light and scanning electron microscopy. Histology revealed new insights on the widely diversified and complex hierarchical assemblage of collagenic structures. Key evolutionary novelties in the organization of sponge connective system were found out. The aquiferous canals are shaped as corrugate-like pipelines conferring plasticity to the water circulation system. Compact clusters of elongated cells are putatively involved in a nutrient transferring system. Knob-ended filaments are characterized by a banding pattern and micro-components. Ectosome and outer endosome districts are the active fibrogenetic areas, where exogenous material constitutes an axial condensation nucleus for the ensuing morphogenesis. The new data can be useful to understand not only the evolutionary novelties occurring in the target taxon but also the morpho-functional significance of its adaptive collagenic anatomical traits. In addition, data may give insights on both marine collagen sustainable applied researches along with evolutionary and phylogenetic analyses, thus highlighting sponges as a key renewable source for inspired biomaterials. Therefore, we also promote bioresources sustainable exploitation with the aim to provide new donors of marine collagen, thereby supporting conservation of wild populations/species.

KEYWORDS
aquiferous canal/cavities system, cellular clusters, connective system and extracellular matrix morpho-functional roles, fibrillar/filamentous/fibrous skeletal structures, Porifera histology/microanatomy

1 | INTRODUCTION

Basic knowledge of sponge collagen-based morphology and morphogenesis of biomaterials (Garrone, 1998) is fundamental in research focusing on sponges as producers of structurally and mechanically interesting biomaterials, such as diversified and abundant collagenic structures (Da Hora et al., 2018; Eherlich et al., 2018; Exposito et al., 1990, 1991, 2002; Heinemann et al., 2007; Langasco et al., 2017; Lim et al., 2019; Martins et al., 2019; Nicklas et al., 2009a, 2009b; Pallela et al., 2012; Pozzolini et al., 2012, 2020; Schröder et al., 2000; Silva

et al., 2014; Tziveleka et al., 2017; Wang et al., 2010). Key points for marine bioinspired technological research are: (i) correct taxonomic identification of target species to standardize processes, (ii) In depth knowledge of functional morphological traits useful for the comprehension of a potential role as biomaterials characterizing body architecture of target species, (iii) exploitation of renewable resources provided by target biomass in the context of a sustainable mariculture and conservation strategies.

In the course of basal Metazoa evolutionary history, Porifera were the first animals able to produce prototypes of an extracellular matrix (ECM), which includes loosely arranged cells. Main components of this ECM are collagenic scaffolds, galectin, and glycoconjugates (Garrone, 1978, 1999; Müller, 1998a, 1998b). Collagenic fibrils are ubiquitous in the mesohyl, and some Porifera branches, that is, Demospongiae without inorganic skeleton (Keratosa), display a great diversification of specialized connective structures embedded in the ground matrix. Since the late 19th century, these soft body architectures intrigued pioneers of sponge studies, namely Gray (1867), Schulze (1878a, 1879b, 1879a,1879b), von Lendenfeld (1889) and Minchin (1900). As the time went by, additional data were provided by numerous researchers (Aouacheria et al., 2006; Bergquist, 1978, 1980; Cowden, 1970; De Cook & Bergquist, 1998, 2002; Erpenbeck et al., 2012, 2020; Exposito et al., 1991, 2002; Gaino, 2011; Garrone 1985, 1999; Garrone et al., 1973; Gross et al., 1956; Junqua et al., 1974; Manconi et al., 2013; Müller, 1998a, 1998b; Müller et al., 2004; Schröder et al., 2000; Sim & Lee, 1999, 2002a, 2002b; Simpson, 1984; Stocchino et al., 2021; Vacelet, 1959, 1971).

Most Demospongiae are characterized with spiculate siliceous skeleton associated with collagenic scaffolds. However, taxa belonging to order Dictyoceratida (subclass Keratosa) are characterized by (a) the absence of endogenous spicules in a network of anastomosing collagenic skeletal elements, which displays a wide range of complexity, and (b) the strategy to trap/incorporate exogenous material from the water column to enhance mechanical support of skeletal fibers and ECM (see Schönberg, 2016; Teragawa, 1986a, 1986b). Moreover, all genera/species belonging to the family Irciniidae share the autapomorphy of peculiar knob-ended filaments (see Bergquist, 1980; De Cook & Bergquist, 2002; Erpenbeck et al., 2012, 2020; Pronzato & Manconi, 2011; Data S1).

The objective of this study was to investigate the organization and function of morphological traits by means of histological analyses of the ECM collagenic architecture of *Ircinia retidermata* (family Irciniidae). Additional information on ECM collagenic structures, supportive of the body architecture in this species, was given by coupling light microscopy (LM) with scanning electron microscopy (SEM).

2 | MATERIALS AND METHODS

2.1 | Experimental model

Ircinia retidermata Pulitzer-Finali & Pronzato, 1980 (Demospongiae: Keratosa: Dictyoceratida: Irciniidae) is a Mediterranean endemic species representing a useful model for investigating the origin and evolution of the connective system architecture in basal Metazoa (see Systematics and geographic distribution, Data S1).

2.2 | Experimental design, study area, and sampling

In order to promote conservation and sustainable experimental mariculture a sponge farming of the target species was utilized as an underwater experimental laboratory, also, with the aim to increase investigations on sponge biology in shallow water (2–3 m depth) and to give support for applied research on blue bioresources, in agreement with the guidelines of the European Commission (2012). Sponge culture plants were harbored in a small marina of Tramariglio Cove (40°35′32.47″N, 8°10′11.50″E; Club Nautico Capo Caccia) within the Capo Caccia—Isola Piana Marine Protected Area (MPA, Northern Sardinian Sea, Western Mediterranean; Ledda et al., 2014; Manconi et al., 2019, 2020; Padiglia et al., 2018; Perez-Lopez et al., 2017; Stocchino et al., 2021).

The identification at species level was carried out utilizing diagnostic morphology and histology usually employed in classical taxonomy. Different histological stainings were applied for LM investigations. SEM allowed 3D-collagenic layout at the level of macro- and micro-structures to be observed.

Representative fragments ($n = 10$) of three experimental clones of *I. retidermata* were collected by means of a scalpel. Live sponges were photographed in the field (EOS G10, Canon, Japan). Samples were immediately kept in seawater in refrigerated bags, and transferred to the Zoology Laboratory, Veterinary Medicine Department, Sassari University.

2.3 | Diagnostic traits and morphological analyses

From 2 to 4 h after the collection, samples were examined using a Leica Wild M3C stereo-microscope.

For taxonomic analyses, samples were washed, dried at room temperature, labeled, registered in reference collections (KER-Sassari University), and differently processed. The morphological diagnostic traits considered for identification of Keratosa up to the species level were as follows: growth form; dermal membrane (surface unarmed vs. armed by exogenous material); conules and oscules (morphometry, shape, and topographic distribution); general skeletal architecture; fine texture of fibrous network; primary, secondary, and tertiary spongin/collagenic fibers (topographic distribution and morphometry); collagenic fibrillar network and filaments (distribution, abundance, and morphometry); ornamentation of fibers; presence and abundance of exogenous material in the pith of fibers.

Thin slices of skeletons were obtained by dissecting samples by hand using scalpels under a Leica Wild M3C stereo-microscope; the slices were then macerated in sea water for a variable time according to the sample size and skeletal texture. After final rinsing and drying

in ethanol, skeletal fragments were laid on a slide, under a weight, to be gently plated as flat thin slices; finally, the sections were cleared in Bio Clear (Bio-Optica, Milan) and mounted in Eukitt® under a coverslip. Observations were made using a Light Microscope (Nikon ECLIPSE 80i, Japan) and photographs were taken with a Nikon Digital-Sight DS-FI camera (Japan). To highlight the skeletal/connective microstructures, skeletal preparations were glued to a stub and sputter-coated with gold and observed by SEM (Tescan Vega3, Czech Republic).

For histological staining, several fragments were fixed at room temperature for 48 h in Bouin's solution, dehydrated in an ascending ethanol series, cleared in xylene, and embedded in paraffin. Sections were cut at section thickness of 5 μm and routinely stained with Masson

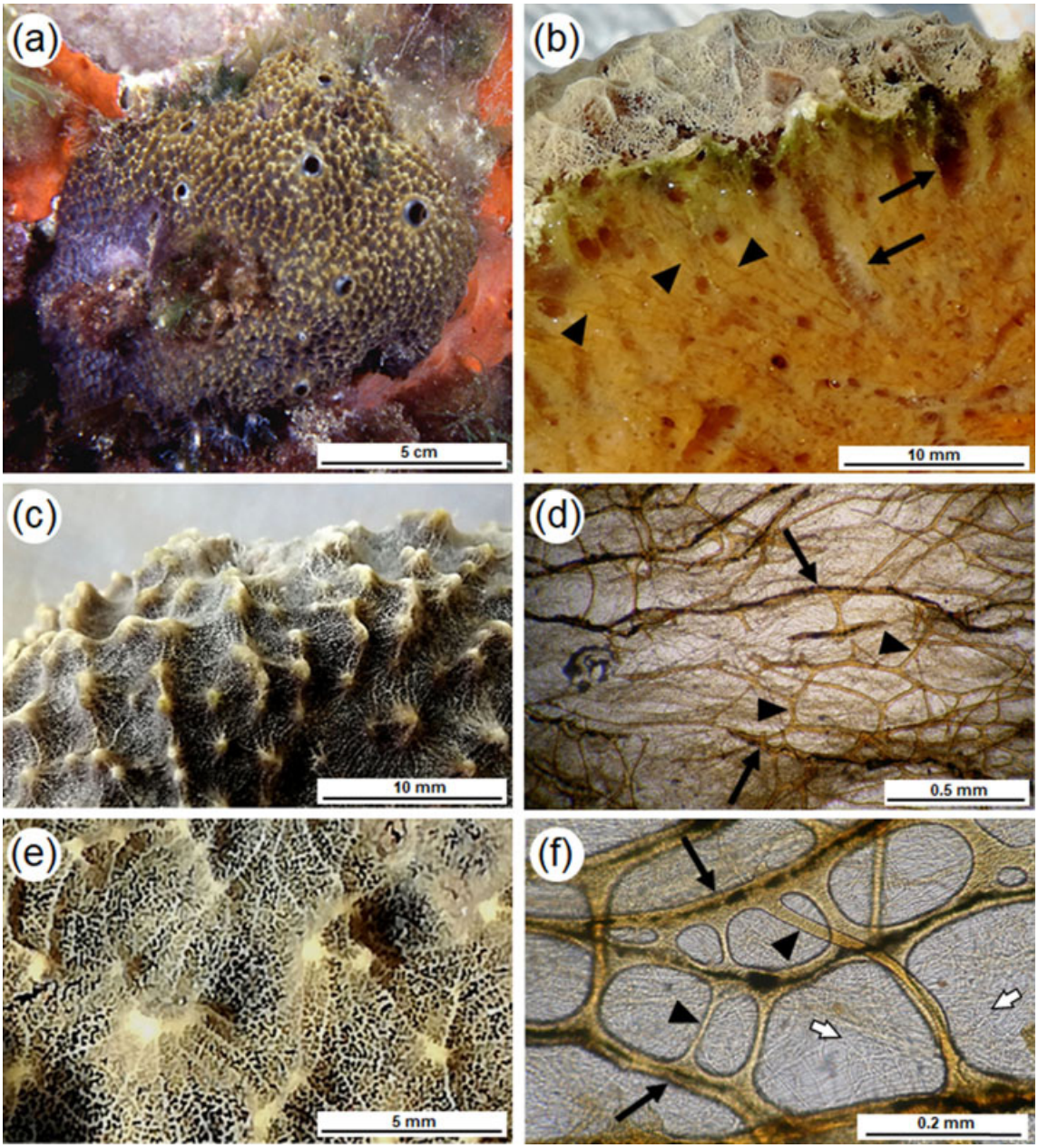

FIGURE 1 *Ircinia retidermata*, growth form and general architecture from an experimental clone in a sponge mariculture plant (2 m depth, northern Sardinian Sea). (a–c, e) macrographs in vivo. (a) Massive brownish to violet sponge with surface bearing variably dense, whitish conules and single, slightly elevated oscules. (b) Body architecture (inner view, cross section) with a dense extracellular matrix yellowish-orange ranging greenish color towards surface, presumably owing to the presence of cyanobacteria. Whitish aquiferous canals (arrows) and orange-brownish ascending skeletal fibers network (arrowheads) also evident. (c, e) Brown interconular surface with fine trellis-like meshwork of inhalant areas among conular prominent tips. Whitish conular tips corresponding to blunt apices of fibers surrounded by star-shaped rays and a network of interconular inhalant areas. (d, f) Micrographs by light microscopy of the main fibrous and filaments network of a macerated and cleaned skeleton (see Section 2). Primary fibers rich of incorporated exogenous material (arrows), connected by an irregular network of secondary fibers free of exogenous material (arrowheads). Abundant dissociated filaments (white arrows) well evident

trichrome and Azan-Mallory trichrome to evaluate the presence and distribution of collagenic structures, and with Alcian blue stain (pH 2.5) to verify the presence of acidic glycans molecules. Slides were examined using a Nikon ECLIPSE 80i (Japan) light microscope and photographs were taken with a Nikon Digital-Sight DS-FI camera (Japan).

The description of the anatomical structures follows the nomenclature of Bergquist (1980) and Boury-Esnault & Rützler (1997).

3 | RESULTS

Ircinia retidermata has a massive and irregular round growth form, varying in size, and forming lobes, each bearing an osculum (Figures 1 and 13). The body surface color varied from beige (in shaded portions) to brownish with whitish conule tips on its rays (Figure 1). Moving inward, a color gradient from light brown/beige to variable shades of orange was evident (Figures 1b and 2a). Some sponges were greenish toward the body surface, presumably because of the presence of still unidentified endobiotic cyanobacteria (Figure 1b). In some ECM ectosomal and endosomal areas, dense assemblages of cyanobacteria were observed (Figure 6e), which will be investigated in a companion paper. Consistency was slightly compressible, elastic, tough, and relatively difficult to tear or cut by scalpel.

3.1 | Collagenic layout of aquiferous canals/cavities architecture

In vivo, at the ectosomal level the sponge surface showed the inhalant area system in the form of a fine trellis-like network located in the interconular spaces and supported by honeycombed meshes (Figure 1b,c,e). Exhalant openings (oscules, 4–7 mm in diameter) were irregularly scattered in variable number with a smooth laminar, variably elevated collar (Figure 1a). Oscular canals and other large ectosomal and endosomal canals were evident as whitish corrugate-like pipelines at their inner surface (Figures 1b and 2a,b). The uplifted inner wall of these canals gave rise to regular prominent annular collagenic structures (Figures 2 and 3). Small canals and cavities were lined by smooth collagenic laminae (Figures 2 and 3).

3.2 | Fibrillar and amorphous layout in the collagenic ECM

The 3D-network of dispersed collagenic fibrils was embedded throughout the ECM of ectosomal and endosomal regions. This network was revealed by Azan-Mallory trichrome as a blue trabecular chondrochyma-like (Figures 3b–d, 5b–d, and 10c). Margins of walls thickening were evident in aquiferous canals and cavities by Azan-Mallory and Masson (Figures 3, and 4a–d). However, at the ectosomal level a fine light blue amorphous homogeneous collagenic material was stained with Masson trichrome (Figure 4a,b).

3.3 | Cellular clusters and collagenic layout

We observed large elongate clusters of cells distinct from the rest of the mostly scattered cells, which were observed arranged lengthwise through the endosomal and ectosomal ECM of *I. retidermata* (Figure 5). Cells were fusiform, rich in granular inclusions, and more highly pigmented than the adjacent cells, and were tightly aligned along densely bundled collagenic fibrils. Each cells cluster was variable in diameter (35–120 μm) and reached up to 10–18 cells per diameter (Figure 5).

3.4 | Collagenic filaments

The 3D-network of collagenic filaments was embedded throughout the ECM of ectosomal and endosomal regions. Filaments were

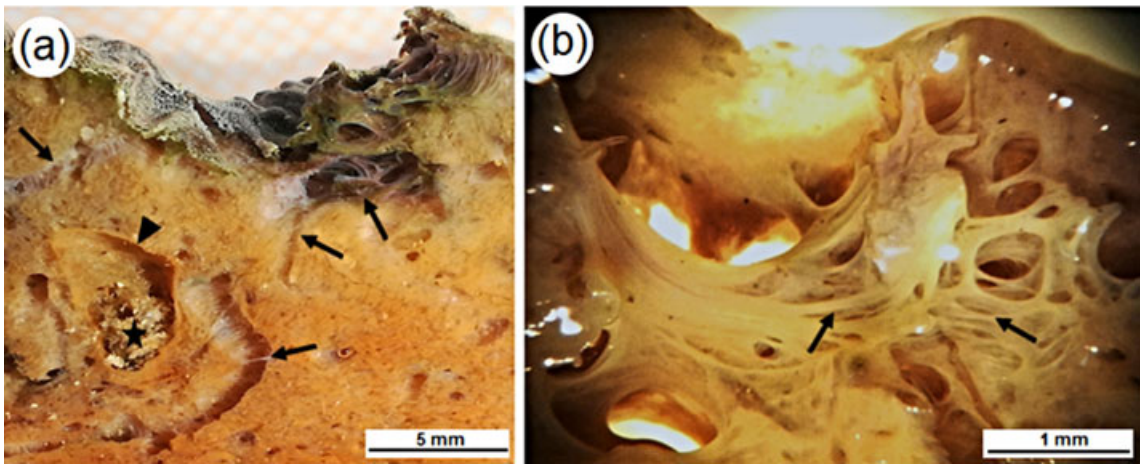

FIGURE 2 *Ircinia retidermata*, collagenic structures in aquiferous canals and cavities. Macrographs in vivo. (a) Corrugated-like laminae (arrows) of pipelines at inner surface of ectosomal canals. Exogenous material (star) within a cavity lined by smooth laminae (arrowhead). (b) Intricate network of stout laminae (arrows) supporting a large oscular canal and lateral subdermal canals

abundant and spatially arranged in the ECM from single scattered to clustered in small ($n = 2–15$) to large bundles up to ~60 (Figures 6 and 11). Filament thickness values ranged ~2–6 μm ($n = 25$ measured) with prevailing thick filaments (Figure 6c–h). Filaments had sub-oval to rounded knob-like tip (~5–18 μm in diameter). With respect to the body biomass, this filamentous network was spatially dominant (>50%). The topographic distribution and the architecture of collagenic filaments extended from endosome to ectosome districts. Filaments tend to aggregate into variably thick bundles that were ascending and oriented from the endosome toward ectosome district (Figures 6b and 13). However, a more complex spatial arrangement was present in the ectosome (see below, Figures 6a and 12).

In SEM, each filament consisted of ~15–30 collagenic fibrils (~200–250 nm in diameter; Figure 7d,e). In addition, SEM analysis also revealed the presence of fibrils belonging to the filament substructure with slightly enlarged button-like end at the tips. These button-like structures were observed emerging from the terminal knobs and along the surface of the filament (Figure 7c,d). A regular transverse banding

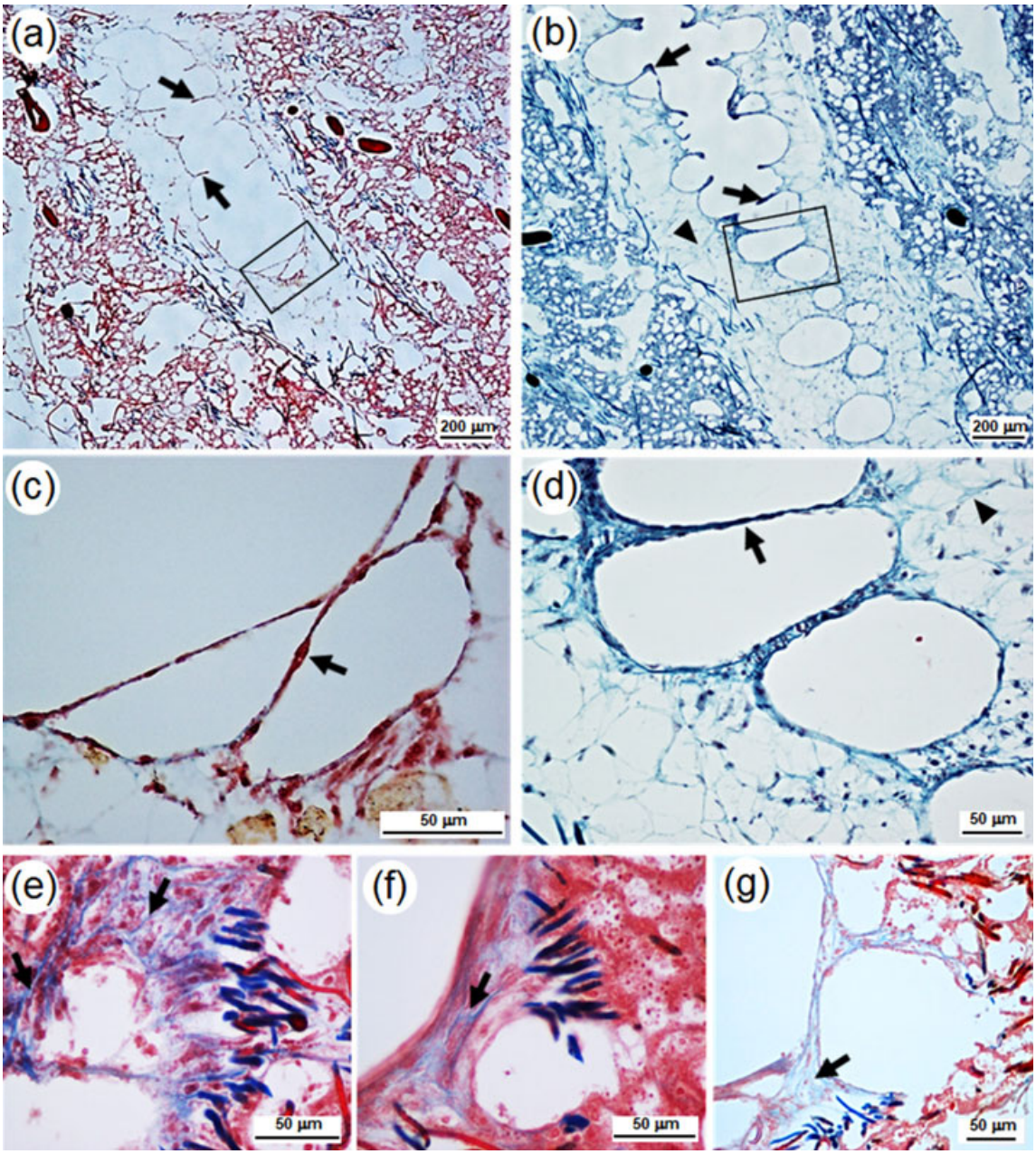

FIGURE 3 *Ircinia retidermata*, collagenic structures in aquiferous canals and cavities (see Figures 1b and 2). Light microscopy micrographs of histological sections. (a–b) Collagenic laminae (endosome) lining the inner wall of canals with regular, annular structures prominent in the lumen (arrows). (c–d) Details of the regions framed in a and b, showing collagenic tie rods lines (arrows) crossing the lumen of canals. Cells along lines sometime evident. (b, d) Chondrochyma-like blue trabecular network well developed (arrowheads). (e-g) Canals/cavities (endosome) surrounded by chondrochyma-like blue trabecular network (arrows) among cells and filament bundles. Masson trichrome (a, c, e–g); Azan Mallory (b, d)

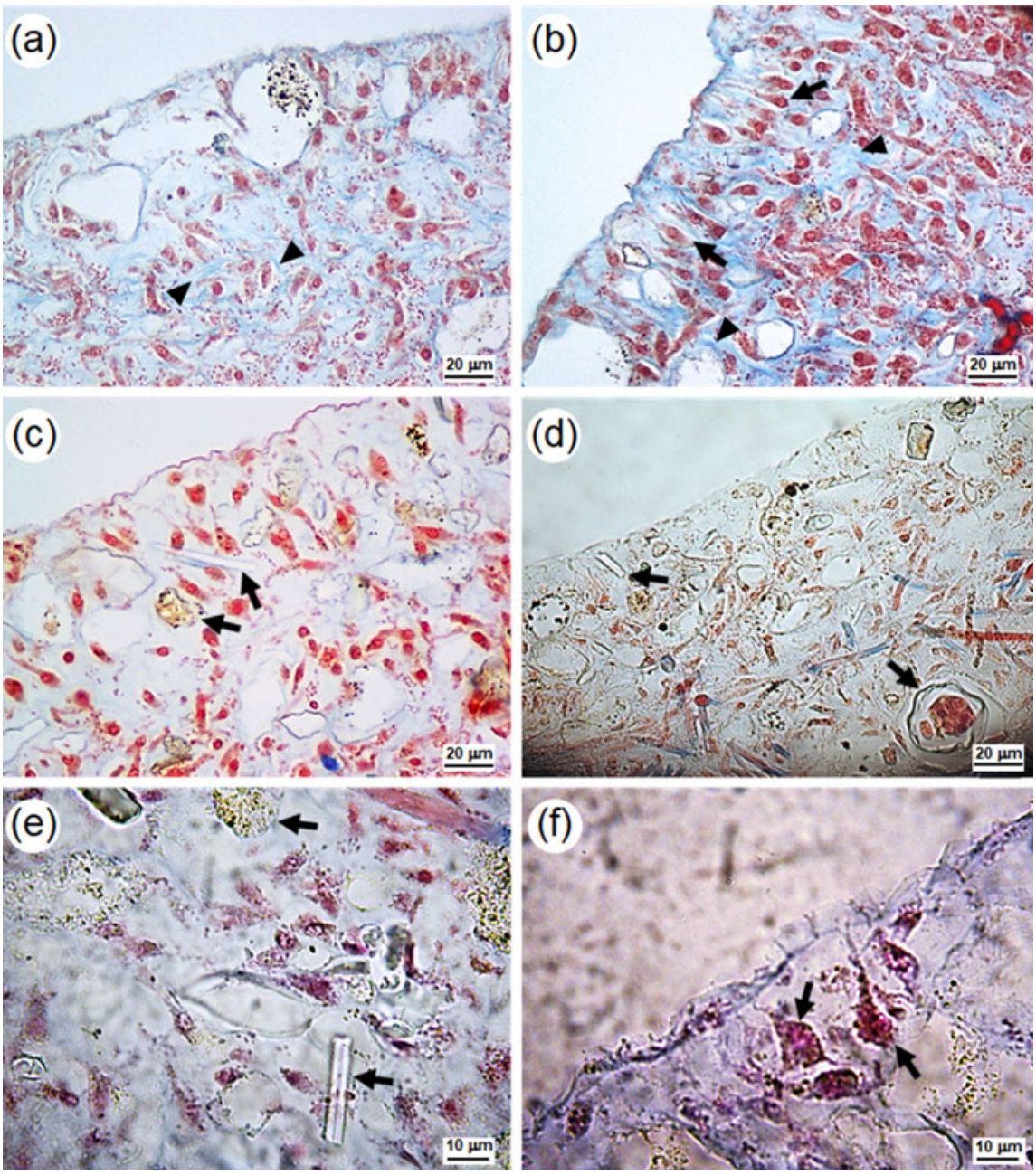

FIGURE 4 *Ircinia retidermata*, fibrillar collagenic network with amorphous texture and cells dispersed in extracellular matrix (ECM). Light microscopy micrographs of histological sections. (a, b) Ectosomal light blue fibrillar network (arrowheads) dispersed in the ECM among cavities/canals together with various cell types. (b) The outermost body surface is lined by the collagenic fibrillar network and exopinacocytes (arrows). (c–e) Exogenous incorporated material (arrows) embedded in the ECM together with ectosomal cells. (f) Cuticle of dermal membrane forming an irregularly fringed layer at outer ectosome with exopinacocytes (arrows). Masson trichrome

pattern with a D-period of ~160 nm was also clearly evident in filaments by SEM (Figure 7c–e).

In LM, the filaments frequently appeared with slightly undulated course, and their terminal knobs were uniformly stained blue with Azan-Mallory trichrome and colorless with Alcian blue. When stained with Masson trichrome, linear portions of filaments were mainly blue to heterogeneously color with prevalent blue alternating with red tracts in the same filament (Figure 6). Some filaments showed blue axial pith surrounded by a thin red layer (Figure 6h). Most knobs had two distinguishable portions. The basal portion of a knob was blue, clearly cup-shaped in some sections, and harboring a red colored apical portion (Figure 6f). In other sections, knobs showed a denser blue spot surrounded by a red area (Figure 6g,h).

Knobs were observed at tips of thick and thin filaments (Figure 6d–h). It was not possible to clearly determine if knobs occurred at both or only one end of a filament. In LM, filaments and knob surfaces carried exogenous inorganic particles appearing translucent with all stainings (Figure 6d,h).

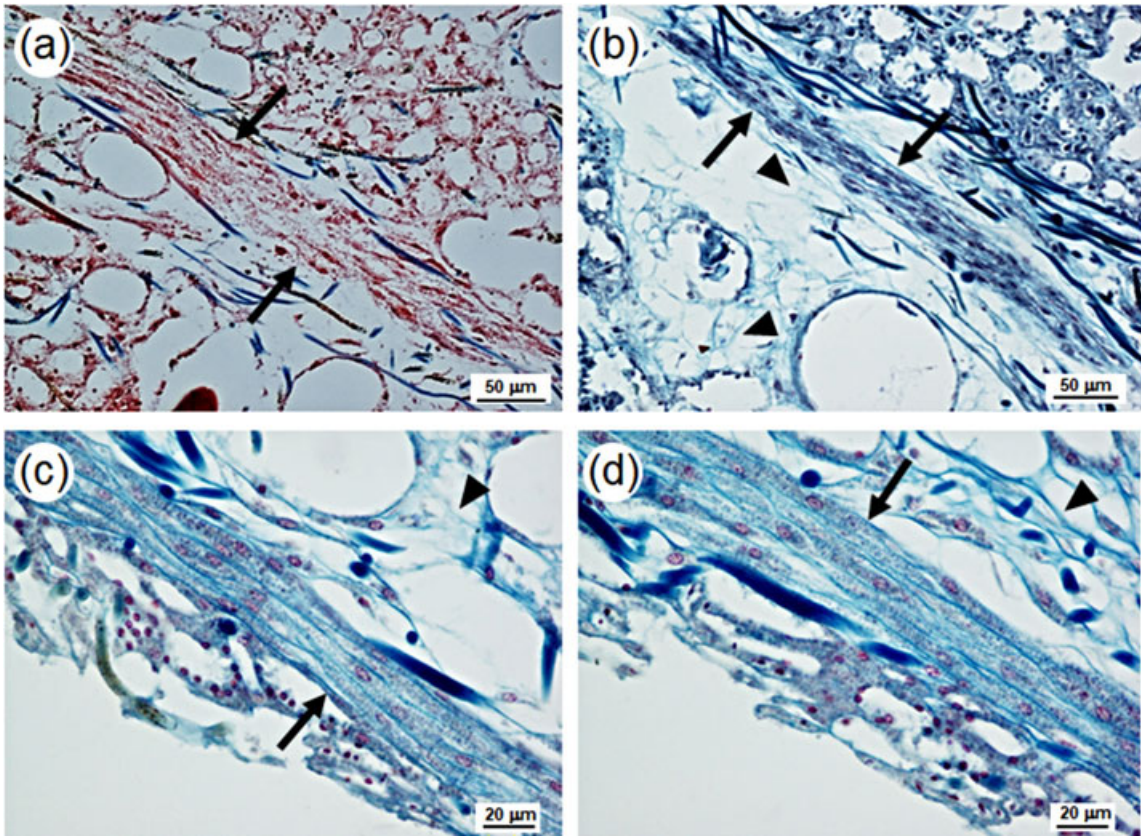

FIGURE 5 *Ircinia retidermata*, cellular clusters (arrows) and filaments in the endosome. Light microscopy micrographs of histological sections. (a–d) Cellular clusters (arrows) of tightly aligned elongated cells. (b–d) Blue trabecular chondrochyma-like network well evident (arrowheads). (c, d) Large nuclei and citoplasmatic inclusions well evident in elongated cells. Masson trichrome (a); Azan Mallory (b–d)

3.5 | Collagenic fibrous skeleton and fiber architecture

The mature fibrous skeleton was light brown to orange in vivo (Figure 1b). It was made up of a reticulate, anisotropic network with irregular polygonal meshes (~230–920 µm in diameter). Primary fibers (~70–100 µm in thickness) were ascending, radial, and more or less parallel joined by irregular intersecting transverse single to anastomosing flattened secondary fibers (~23–90 µm in thickness; Figures 8a–d and 11b,c) sometimes perforated by holes variable in density and size, like cribrose plates (Figure 9a,g).

Main fibers (primaries) ranged along their length, in ectosome and endosome districts, from cored by exogenous material to less frequently uncored. Detritus irregularly embedded in the fibers pith as main axis (core) in a wide range of morphology, density, and granulometry (~12–115 µm in diameter; Figures 8, 9, and 10).

Mature fibers, made up of the bark surrounding the pith, were morphologically heterogeneous along their length. Their surface consisted of bark layers ranging from entirely smooth to variably rough because of the heterogeneous occurrence of exogenous material embedded in the pith (Figures 9 and 10). The blue axial pith (Masson and Azan-Mallory) was surrounded by a variably developed multilayered bark (red with Masson, blue with Azan-Mallory and colorless with Alcian blue; Figures 9 and 10). The axial pith ranged from amorphous when not cored to irregularly/partially laminate when harboring exogenous material (Figures 9 and 10). However, in most cases only the footprint of inclusions was observable in sections. Very likely, exogenous grains were lost during the fixation and slicing processes. Sometimes blue-turquoise material was evident with Alcian blue in the pith of cored tracts of fibers indicating the presence of acidic glycans (Figure 10g). However, the uncored fiber tracts were colorless.

The transition between laminated bark and pith was distinct (Figures 8, 9, and 10) and the bark occupied up to more than 50% of the fiber diameter in secondary fibers and in fibrous tracts of primaries lacking inclusions (not cored).

The bark was seen to be made up of dense, concentric almost adherent laminae (growth lines). Moreover, an amorphous matrix (blue with Masson trichrome and Azan Mallory, colorless with Alcian blue) was present between the bark layers that are not always strictly compacted (Figures 8, 9, and 10). Plated secondary fibers, sometimes cribrose, showed the same collagenic structural layout and composition as the primary fibers (Figure 8).

3.5.1 | Fiber morphogenetic processes

All traits of mature fibers, recognized both by staining and morphology, correspond to formations that we interpreted as successive phases of fiber maturation. These phases occurred in adult sponges at the ectosome and outermost endosome districts (Figure 10). The early

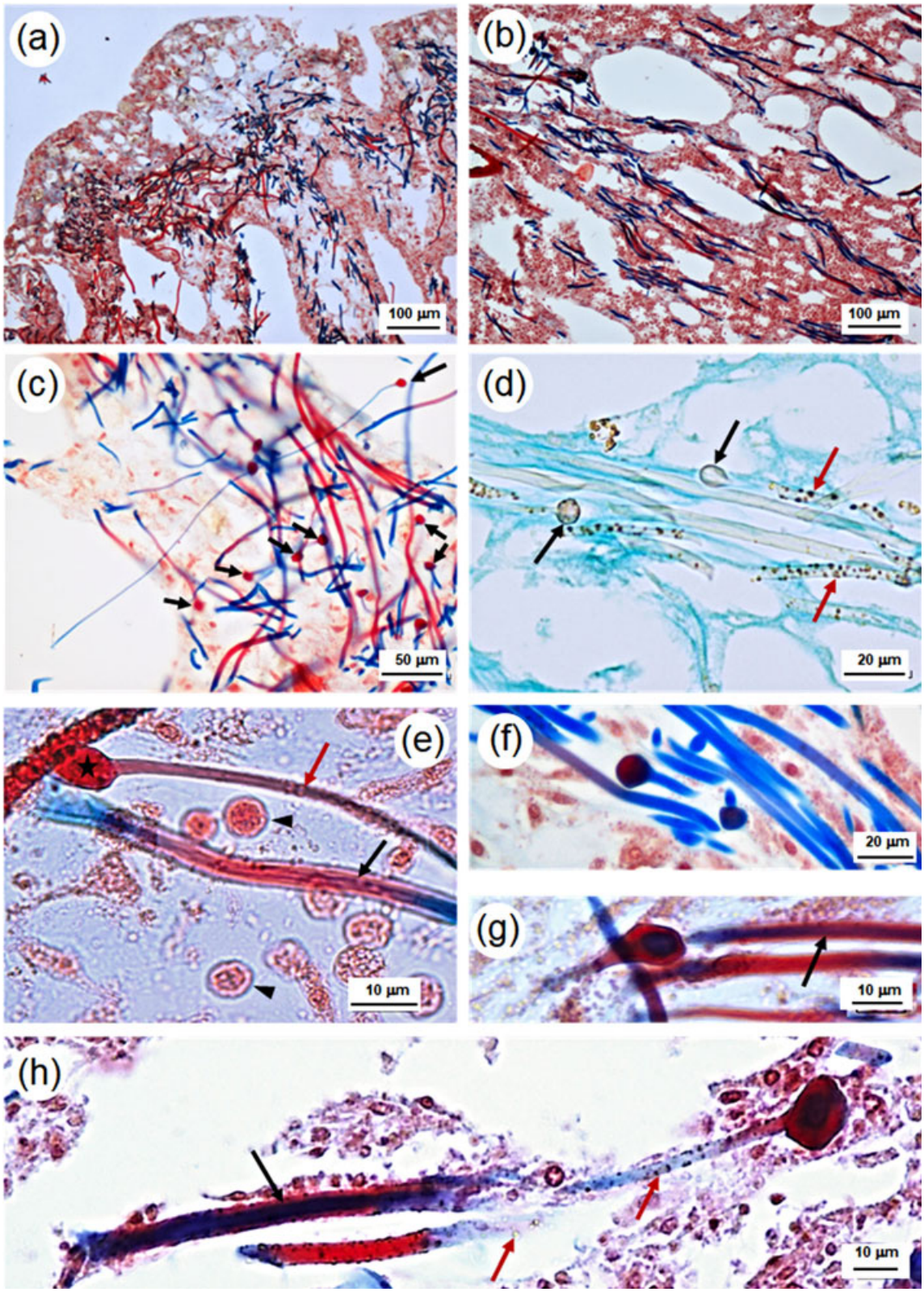

FIGURE 6 *Ircinia retidermata*, collagenic filaments. Light microscopy micrographs of histological sections. (a, b) Topographic distribution and architecture of filamentous network (blue to red) of ectosomal and outer endosomal regions (a) and of choanosome (b). (c) Knob-ends (arrows) of thin and thick filaments from blue to red. (d) Colorless knob-ends of filaments (black arrows). Exogenous inorganic particles also clearly visible along filaments (red arrows). (e–h) Various morph and color shown by knob-ended filaments. (e) Longitudinal section of three different filaments: red knob (star) of a thin filament (red arrow); thick filament with denser axial pith (black arrow); red filament (top, left) with exogenous inorganic particles. Cyanobacteria also present (arrowheads). (f) Blue filaments with red knobs delimited by a blue rim. (g,h) Zoomed view of filaments (black arrows) with a denser blue axial pith and red knobs including a blue central area. Exogenous inorganic particles (red arrows) clearly visible (h). Masson trichrome (a, b, c, e, f, g, h); Alcian blue (d)

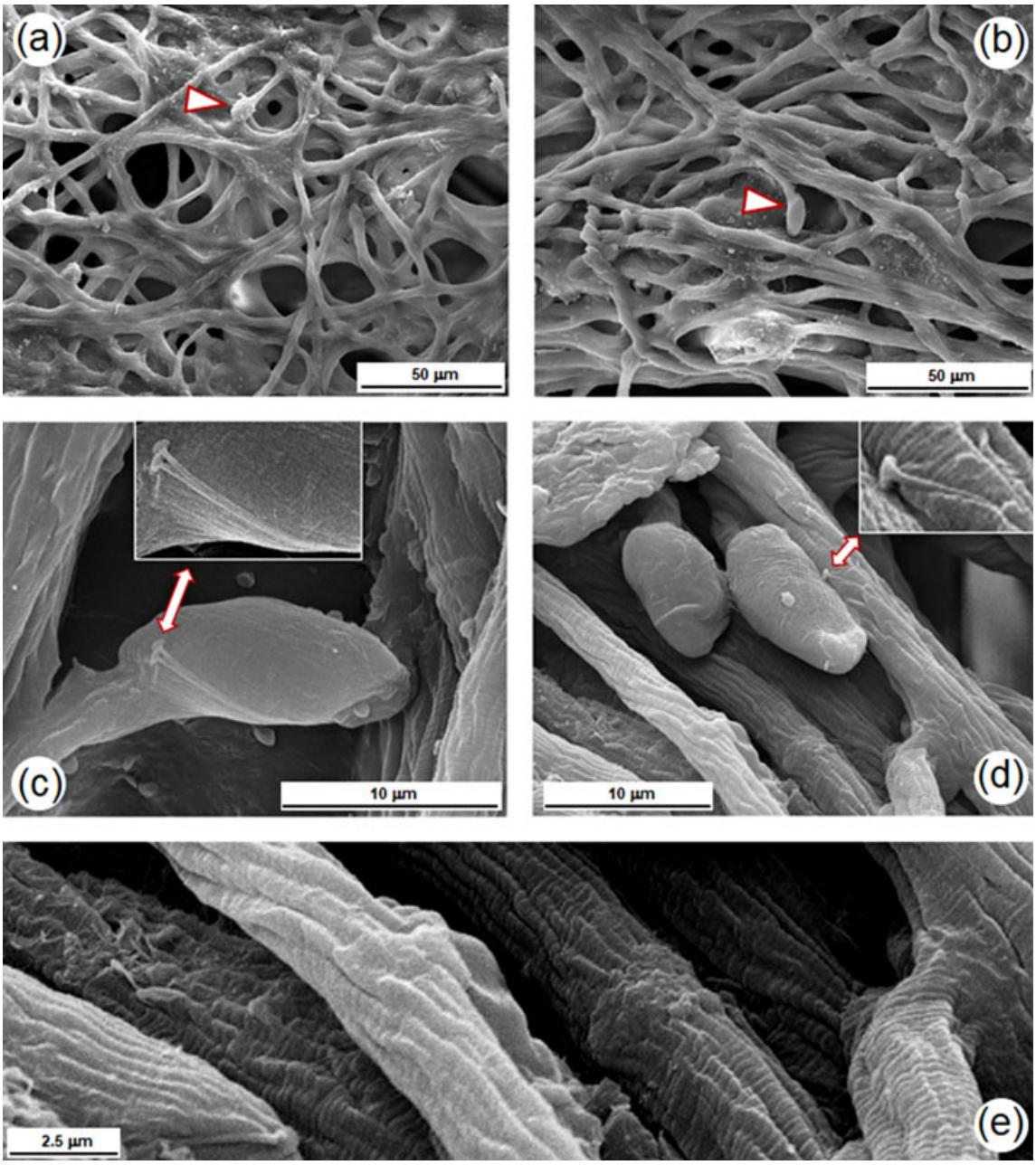

FIGURE 7 *Ircinia retidermata*, collagenic filaments at the ectosome. Scanning electron microscopy micrographs after sponge seawater maceration. (a–b) Dense meshwork of filaments with sub-oval knob ends (arrowheads). (c, d) Sub-oval knob-ended filaments (zoomed view in the insets). Microfibrils distally enlarged to form a button-like tip (arrows), which emerges from both knob end (c) and filament surface (d). (e) Banding pattern highlighting the sub structural layout along the wrapped surface of filaments

developmental phase started around an axial mass of exogenous detritus grains acting as the condensation nucleus, which drives the neo-pith formation (Figure 10a). Grains of this nucleus were heterogeneous ranging from sand and allochthonous sponge spicules to vegetal detritus and diatoms frustules (Figures 9 and 10). Single grains or group of grains embedded in ECM were uniformly surrounded by dense cell masses composed of spongocytes secreting amorphous collagenic material (blue with Masson and Azan Mallory; Figure 10a–e).

In intermediate developmental phases, the axial material (neo-pith) was surrounded by irregular to partially laminate collagenic layers (blue with Masson and Azan Mallory, Figures 9 and 10). In advanced growth phases occurring outward, we observed spotted red collagenic masses corresponding to the neo-bark formation at the blue outer surface of the pith (Masson, Figure 9). Sometimes cells were also observed within the growing neo-pith (Figures 9b,d and 10b,d).

Spongocytes, lacking secretive granules, ranged from fusiform to polygonal in shape (Figure 10). Their peripheral cytoplasm was well defined when compared with the other cells scattered in the ECM (Figure 10). No spongocyte masses were observed around mature fibers (Figure 10f).

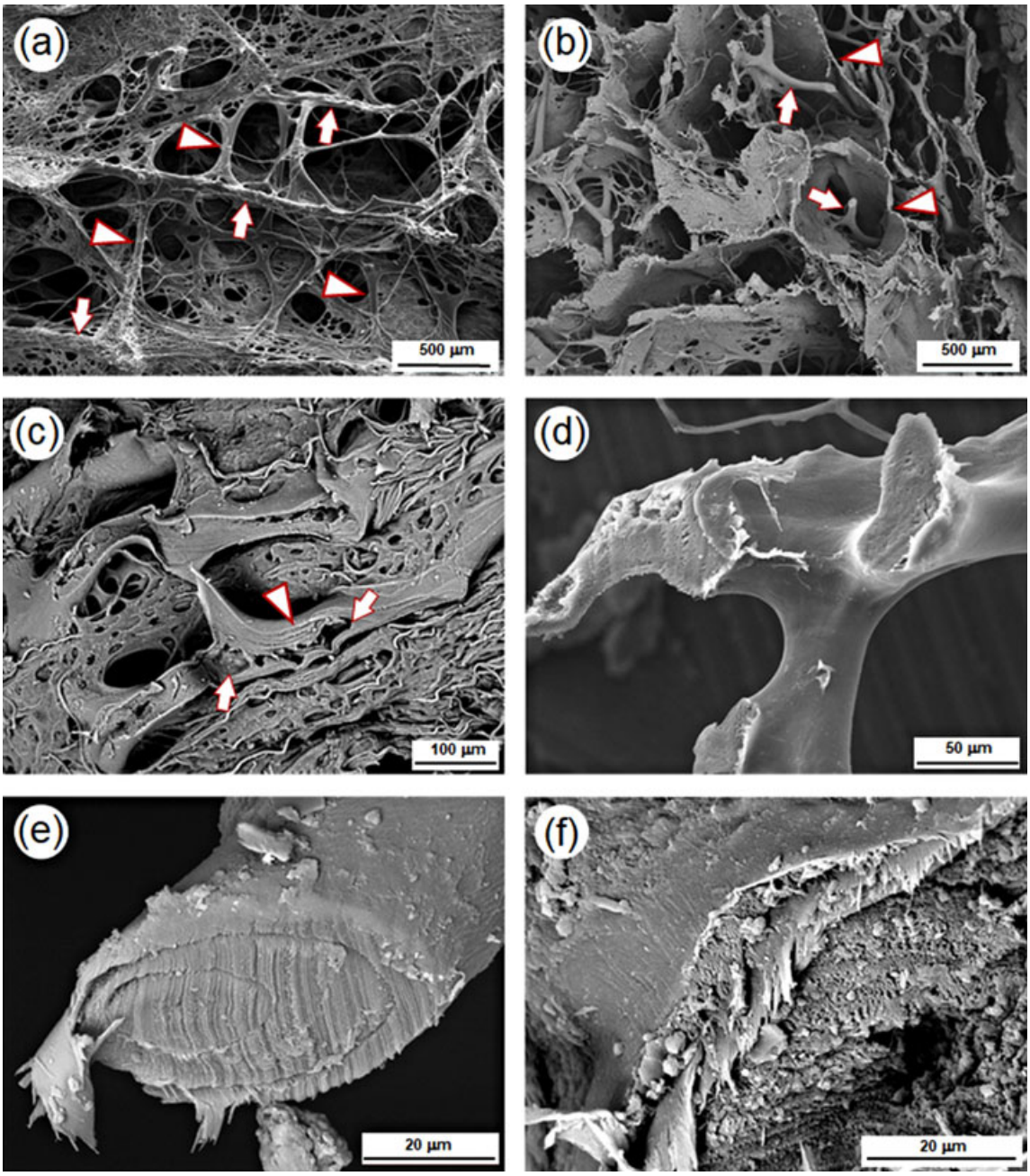

FIGURE 8 *Ircinia retidermata*, hierarchical architecture of fibrous skeletal network. Scanning electron microscopy micrographs after sponge seawater maceration. (a) Reticulate anisotropic network with three parallel main fibers (arrows) joined by numerous thinner, smooth secondary fibers (arrowheads). Irregular surface of main fibers is due to the axial incorporation of exogenous material. (b) Filamentous laminar structures (arrowheads) along subdermal canals surrounding thin, smooth, plated secondary fibers (arrows). (c) Parallel primaries joined by perforated plated secondaries. Longitudinal view of layout along a main fiber with a concentrically multilayered bark (arrowhead) surrounding the pith mainly occupied by axial exogenous materials or their footprints (arrows). Large bundles of filaments evident. (d) Flat secondaries fibers joining to form a cribrose plate (cross section). (e) Sub-oval outline of a secondary fiber (cross-section). (f) Longitudinal concentric fibrillar laminae of the bark surrounding the central pith (cross-section)

3.6 | Architecture of the complex collagenic ectosome and exogenous material incorporation

The outer body surface was conulose at variable density in different areas. Conular dimension decreases from top toward the basal sponge portion. Conules were from single to group in lines (~1–3 mm apart). Conules (~1–2 mm in height) with variably blunt apices had a conular axis made by distal parts of primary fibers; sometimes fiber tips were bare and protruded from apices (Figures 1c and 11). The interconular areas were covered by a honeycombed network of meshes (~0.80–1.5 mm in diameter), which conspicuous at bare eye (Figures 1, 11, and 12).

The three dimensional structure of the ectosome showed a network-like hierarchical architecture ranging from fibrous to filamentous. The cuticle/hyaline membrane (light blue with Masson and Azan Mallory trichrome,

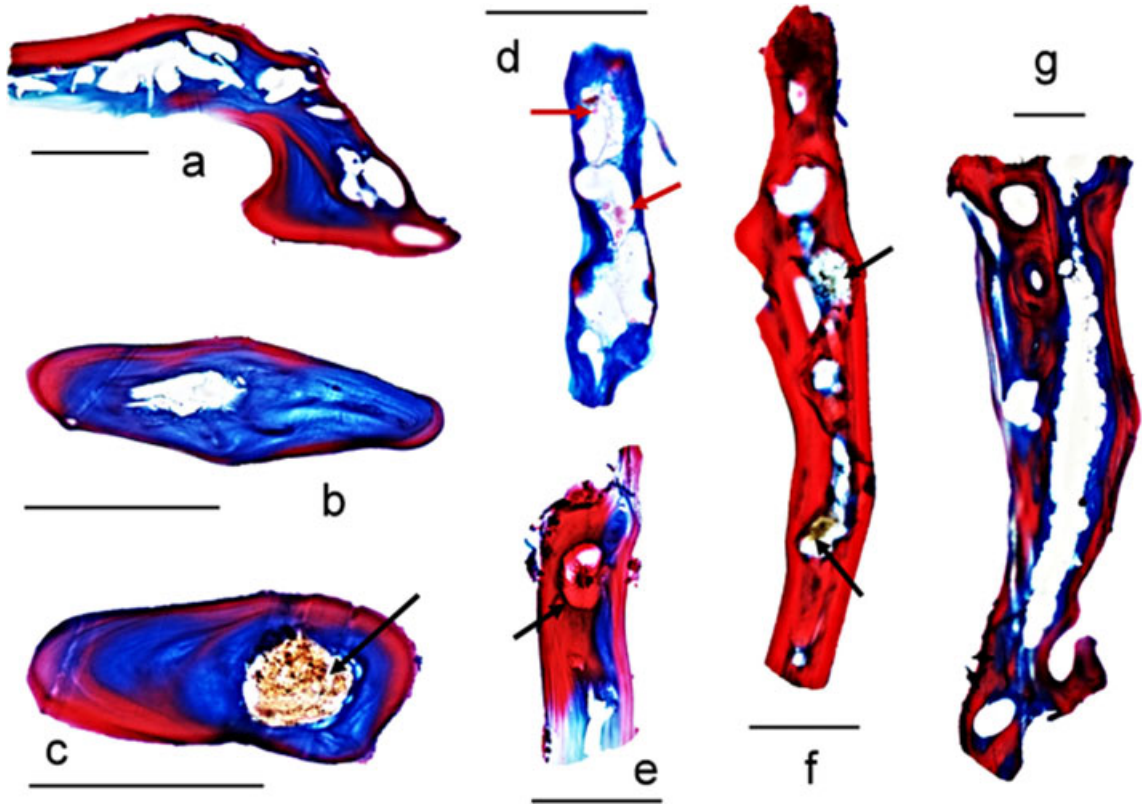

FIGURE 9 *Ircinia retidermata*, collagenic architecture of skeletal fibers. Axially arranged exogenous inclusions, for example, sand grains, spicules, organic material (black arrows), or their footprints evident in the pith. Also cells (red arrows) sometimes evident in the pith. Light microscopy micrographs of histological sections. Scale bars 100 μm. (a) Fibrous plate (longitudinal section) with concentrical multilayered bark (red) surrounding the pith (blue) and axial footprints of exogenous inclusions. Extended blue areas suggest a growing process. (b, c) Fibers with blue pith surrounding inclusions (arrow) and outer red bark (cross sections). (d) Blue young growing fiber (longitudinal section) with a few small, scattered spots of red neo-bark at the outer surface. Residual cells (red arrows) evident in the pith. (e) Fibrous plate with red bark and blue pith (longitudinal section). Tubercled exogenous spicule (arrow) embedded in the pith. (f) Fiber with well-developed red bark, and axial inclusions (arrows) embedded in the blue pith. (g) Fibrous plate with rounded holes and large, irregular footprints of granular inclusions within the blue pith (longitudinal section). Masson trichrome

blue turquoise with Alcian blue) was an acellular cribrose lamina smooth and very thin (<1 μm). Hyaline membrane ranged from smooth and thick (Figure 4) to fringed and thin due to the loss of the detritus crust during sample processing. The underlying layer was cellular and composed by pigmented T-shaped exopinacocytes (Figure 4). The ectosomal ECM was armed by exogenous detrital micro-grains more or less embedded and irregularly distributed with topographically variable density and granulometry, that is, sand, spicules, diatom frustules, and vegetal material (Figure 4).

Under this outer layer (Figure 4) an almost radial irregularly dense filamentous meshwork was evident in vivo and in SEM (Figures 1 and 12). This meshwork, supported by the distal portion of axial skeletal fibers, was made by a thin network of filaments in between a few ($n = 3–5$) thick radial filament bundles. This network was visible in LM histological sections of the ectosome only here and there, owing to the sections of the filamentous meshes composing the 3D-reticulum (Figure 6a). The same filamentous 3D-network appeared collapsed in SEM after complete seawater maceration (Figure 12b,d–f).

The fibrous ectosomal skeleton was composed of dense, ascending fibers; growing ectosomal fibers were observed at various developmental/morphogenetic phases (Figure 10a–e). Ectosomal ECM in histological sections appeared intensively turquoise colored by Alcian Blue indicating high amount in acidic glycans. The ECM was less turquoise colored toward sub-ectosomal and choanosomal level.

3.7 | Overview of the architectural organization

To improve the comprehension of the complex architecture of the *Ircinia retidermata* body, a model overview section is provided to give evidence of its general organization (Figure 13). Body districts were magnified to focus the topographic distribution of ectosome, endosome, aquiferous system, and skeleton from filamentous to fibrous. These structures were shown at different level of detail.

4 | DISCUSSION

4.1 | Sponge collagenic material from sustainable source

The present morphological research is based on sustainable sponge mariculture (Pérez-López et al., 2017) as experimental sea-based

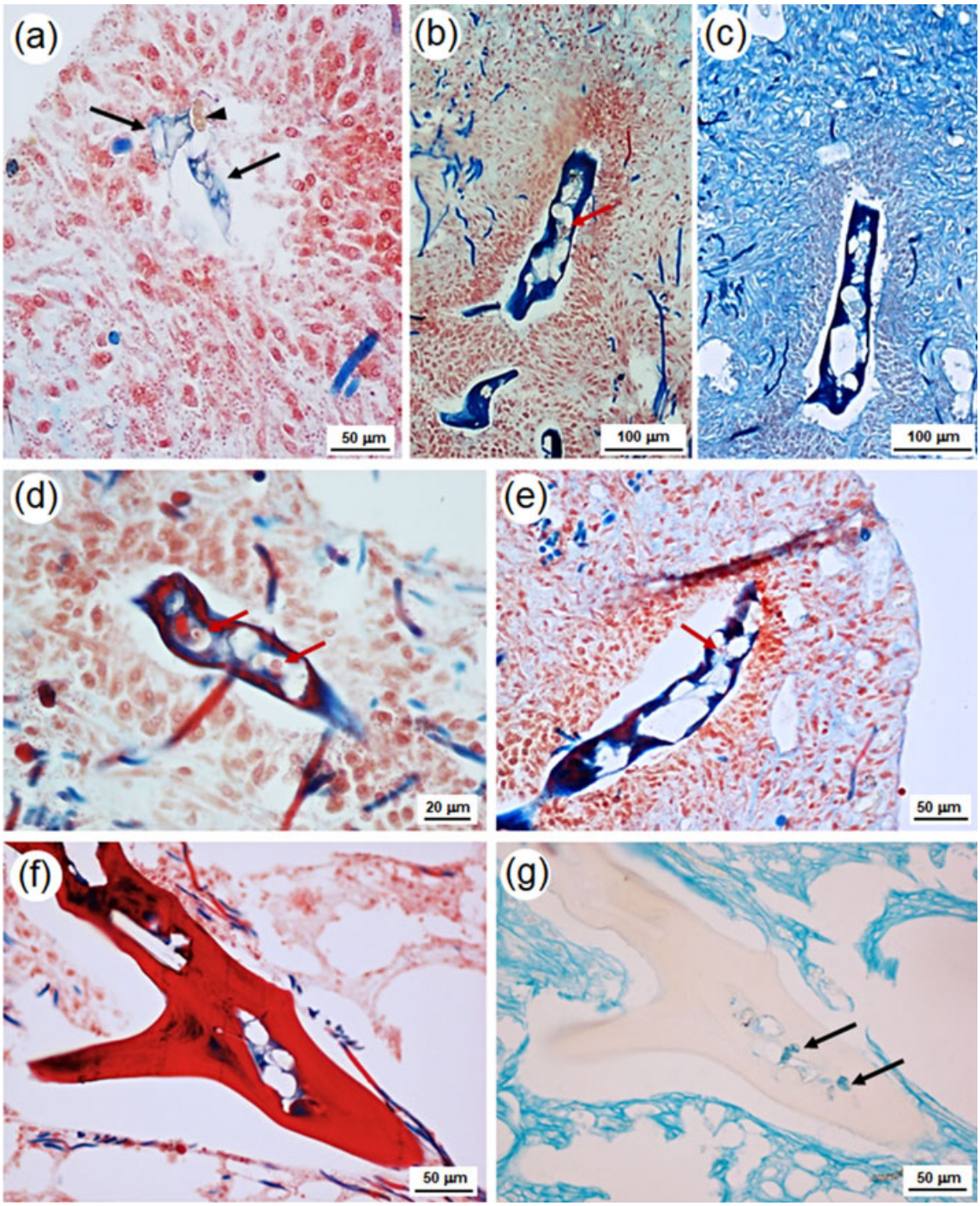

FIGURE 10 *Ircinia retidermata*, fiber morphogenesis in the ectosome and outer endosome. Secretive phases of collagen around the granular exogenous material as condensation core of the neo-pith, with subsequent collagen assemblage to form the neo-bark. Light microscopy micrographs of histological sections. (a) Dense masses of spongocytes in secretive phase showing piriform to polygonal outline in the ectosomal extracellular matrix. A thin bluish collagenic layer (arrows) uniformly surrounds axial grains (arrowhead). (b) Spongocytes around a growing primary fiber with axial grains (red arrow) embedded in the blue neo-pith. (c) Growing fiber immersed in the trabecular chondrochyma-like network. (d, e) Growing fiber including cells (red arrows) in the neo-pith together with footprints of exogenous material. (f, g) Different staining of the same mature fiber shows a thick bark (red in f vs. colorless in g) with a residual presence of light blue acidic glycans (arrows) in the pith. Masson trichrome (a, b, d, f); Azan Mallory (c); Alcian blue (g)

laboratory. This supply of biomass for marine collagen basic research, and its applications in bioinspired materials science and technologies, is in agreement with eco-friendly bioresources management and sustainable exploitation following the global strategy of marine biodiversity conservation plans to preserve wild populations/species and their ecosystem services (de Caralt et al., 2003; Gökalp et al., 2021a,

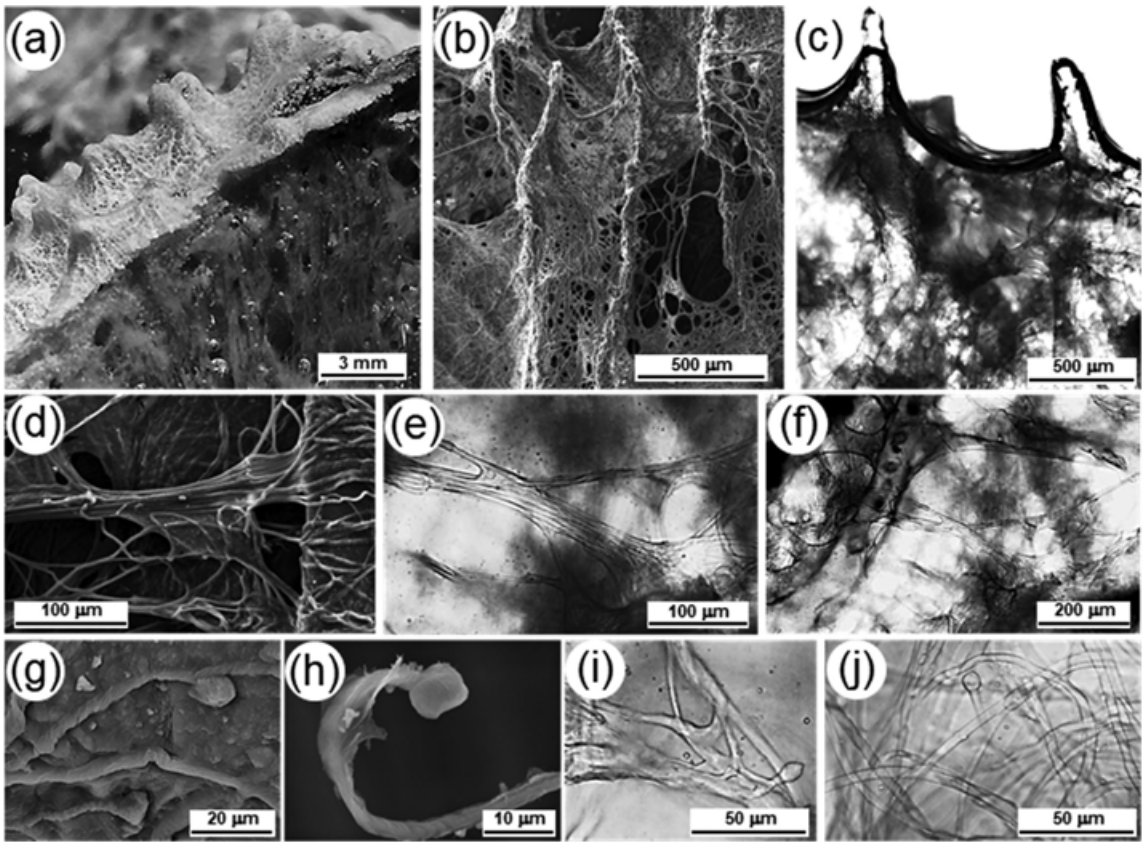

FIGURE 11 *Ircinia retidermata*, ectosomal complex layout with skeletal networks of fibers and knob-ended filaments. Photomicrographs in vivo (a), light microscopy in various phases of seawater maceration (c, e, f, i, j) and scanning electron microscopy (b, d, g, h). (a) Ectosome in toto witj singly/grouped conules among interconular trellis-like inhalant areas showing rounded/polygonal meshes. Whitish color of this micronetwork is due to finely dusty incorporated exogenous material. (b) Distal portion of ascending primary fibers supported by arched/plated secondaries fibers in a dense collapsed filamentous network. (c) Conular apices supported by fibers and filamentous network. (d–f) Networks of filament bundles between skeletal fibers. (g–j) Knob-ended filaments

2021b; Murray et al., 2013; Orel et al., 2021; Padiglia et al., 2018; Pérez-López et al., 2017; Pronzato, 1999; Pronzato et al., 1999; Ternon et al., 2017; Wanick et al., 2015, 2017). The long-time evolutionary success of our model sponge with exclusive collagenic body architecture, together with its shallow water habitat (wild and farming conditions), suggests also a potential great ability of Irciniidae to adapt to climatic changes and to face constraints represented by global warming, ocean biogeochemistry, and ocean acidification.

4.2 | Fibrillar collagenic network in the ECM

In *Ircinia retidermata*, a dispersed fibrillar collagenic network is extended throughout the ectosomal/endosomal ECM, as in most demosponges (Ereskovsky & Lavrov, 2021; Simpson, 1984). These structures mediate cell-matrix interactions via membrane receptors regulating cell behavior (Exposito et al., 2002; Müller, 1997) and contribute to build the architecture of the (a) chondrochyma-like trabecular networks (Cowden & Harrison, 1976; sensu Minchin, 1900; Stocchino et al., 2021), and of (b) walls thickening of aquiferous canals and cavities.

In the aquiferous canals, the corrugate-like pipelines and their annular formations, which confer plasticity to the system, seem to be evolutionary adaptive traits involved in supporting: (a) water flow vorticity to facilitate access to nutrients and gas exchange by epithelial cells; (b) water pumping activity and physiological rhythmic variations in the extent of flow rate; (c) contraction/expansion and water flow direction.

It is known that in general the fibrillar network represents a substrate along which occurs the movement of cells. Collagenic fibrillar network also extends among elongate clusters of cells in our samples of *I. retidermata*. The functional role of such structures is still unknown. However, these cells clusters closely resemble the strand of cells found until now exclusively in the genus *Aplysina* (Ereskovsky & Lavrov, 2021; Leys & Reiswig 1998), where these cells have a permanent position along the strands and do not actively move. According to Leys & Reiswig (1998, p. 40) the role of these cells

> is primarily to bundle and align the collagen fibrils, creating a pathway that the cells transporting nutrients can recognize and follow, thereby allowing the rapid transport of material to the tip or to the base of the sponge

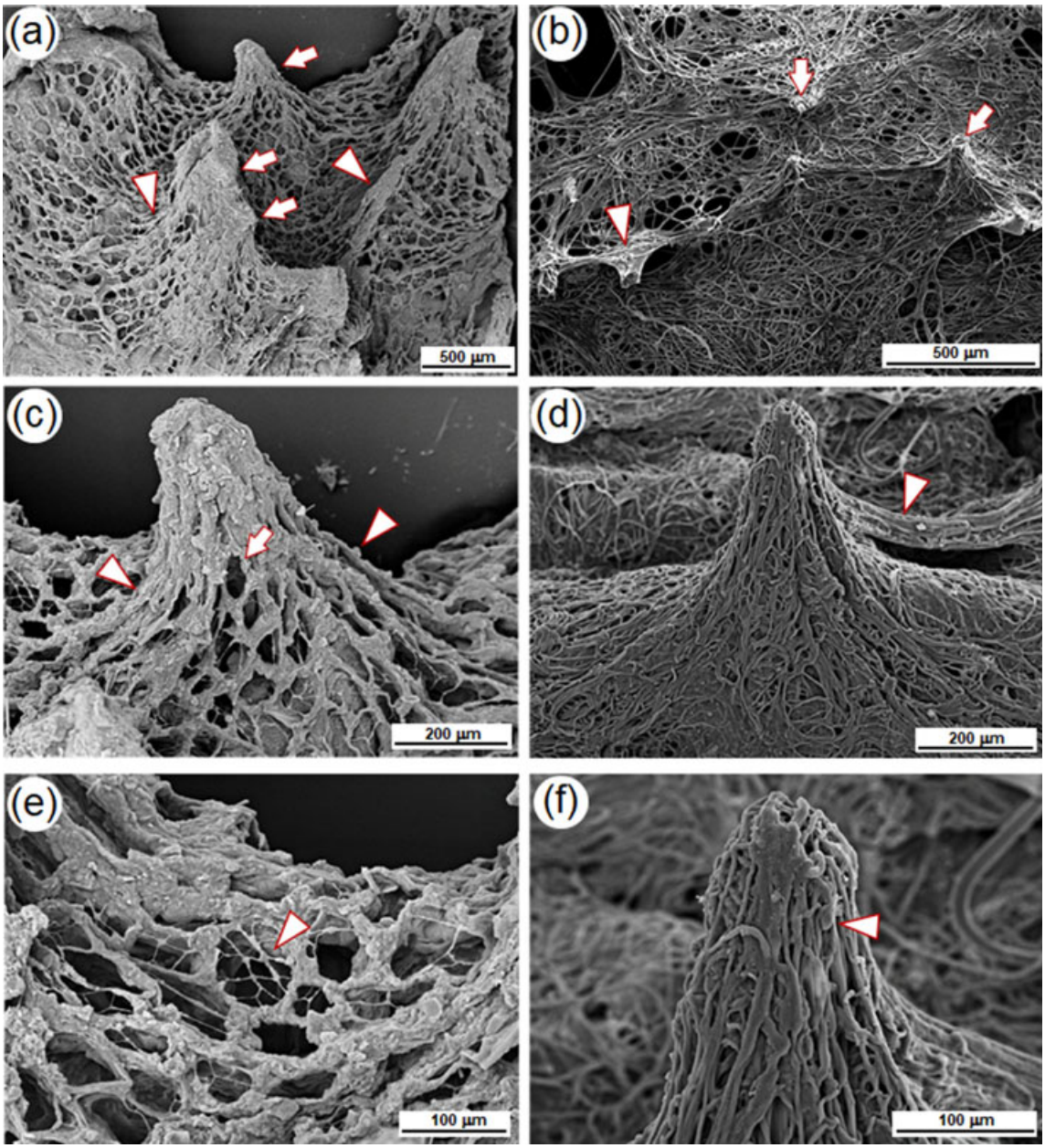

FIGURE 12 *Ircinia retidermata*, ectosome with hierarchical architecture of collagenic fibers, filaments, and filamentous laminae. Scanning electron microscopy micrographs. (a) Outer layer of conular area with conules singly scattered or grouped in variably oriented dense rows (arrows). Radial stout rays (arrowheads) surround each conule. (b) Arched secondary fibers (arrows) and flattened cribrose fibers (arrowhead) supporting a dense filamentous network (top view). (c) Network of rounded/polygonal meshes (arrow) overlaying a conule and adjacent interconular areas (arrowheads). (d) Zoomed view of a conule densely overlaid by filaments. Stout rays well evident (arrowhead). (e) Detail of trellis-like micronetwork (arrowhead) in honeycombed mesh of interconular area. (f) Magnification of knob-end filament tip (arrowhead; detail of d). (a, c, e) after short seawater maceration; (b, d, f) after long seawater maceration

and

> are suggestive of a primitive nutrient transport pathway in sponge.

We follow these ideas and suggest that the cellular clusters of *I. retidermata* are part of the nutrient transport system towards sponge body districts.

4.3 | Collagenic filaments

Banding pattern and a D-period of ~160 nm is clearly evident in *I. retidermata* on surface of collagenic knob-ended filaments by SEM (Figure 7). A repeated band periodicity has been reported mostly for fibrillar collagens (e.g., Exposito et al., 2002; Garrone et al., 1975; Müller, 1997; Müller et al., 2004) and among Keratosa for *Ircinia fusca* (Carter, 1880) (see Pallela et al., 2011, Figure 7). The peculiar fibrils

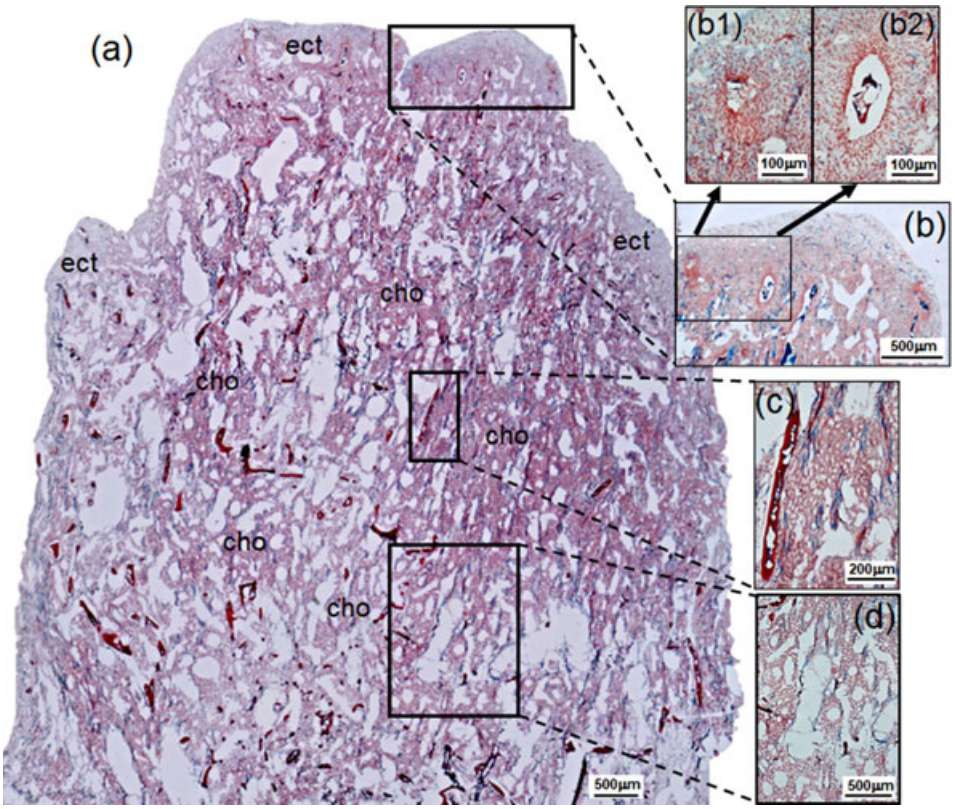

FIGURE 13 *Ircinia retidermata*, overview of architecture and topography of framed body districts at different level of detail (boxes). Light microscopy. (a) General view of ectosome, choanosome, aquiferous system (d box), and filamentous/fibrous skeleton (b–c boxes). (b) Ectosomal morphogenetic area in growth phase. (b_1-b_2) Details of inorganic axes of neo-fibers surrounded by spongocytes secreting collagenic material. (c) Endosomal district with filament bundles and a mature fiber cored by inorganic exogenous material. (d) Large corrugated canals of the aquiferous system in the endosome district rich of choanocyte chambers. Masson trichrome. Ect, ectosome; Cho, choanosome

with button-like tips belonging to the filament substructure are firstly reported.

The particles which are translucent with all staining and occurred on filaments are of unclear origin and nature. However, considering their resemblance with the iron granules found in the fibers of other Keratosa (Spongiidae) by Kenneth & Rützler (1968) and Vacelet et al. (1988) it could be possible suggest a mineral origin also for these particles. The absence of these latter particles in the SEM samples could be due loss during/after maceration processes.

Collagenic organization of filaments and terminal knobs is heterogeneous in *I. retidermata*. The occurrence of different staining (with Masson trichrome) in different filaments and/or in various portions (outer layer and axial pith) of the same filament supports the structural heterogeneity of their collagenic components. The structure of *I. retidermata* filaments matches data reported for genus *Ircinia* by Garrone et al. (1973, fig. 1, p. 257)

> These filaments consist of three layers: a cuticle-like outermost layer, a soft cylinder (forming the bulk of the filament) within this tubular cuticle, and an axial thread in the center. With electron microscope the filaments appear as bundles of microfibrils (about 50 to 70 Å in diameter) twisted in a helical fashion, nearly straight in the axis of the filament and becoming increasingly coiled toward the periphery.

In addition, this architecture and staining resembling those of fibers in *I. retidermata* also partially matches the delineation of Irciniidae filaments as small spongin fibers as reported by several authors (Brien et al., 1973; Gaino, 2011; Garrone et al., 1973; Simpson, 1984). However, in *Sarcotragus spinosulus*, which also belongs to Irciniidae, filaments were always homogeneous and only blue when stained with Masson (Stocchino et al., 2021).

The presence in *I. retidermata* of thin and thick filaments portions and the fact that it was not possible to determine if knobs occurred at both or only one end of a filament, suggests three possible filament morphologies: (a) two types of filaments, thin and thick each with a single knob end; (b) two types of filaments, thin and thick each with two knobs ends; (c) a single type of filament, ranging along its length from thin to thick, with one knob at each end. Notwithstanding numerous investigations on filaments, their morphological divergence in different species and/or their plasticity in the same species along with the functional role of their diversity continue to be unresolved. Additional comparative studies are necessary in order to shed light on these skeletal components.

From a functional point of view, the abundance of filaments bundles and their spatial arrangement in networks of irciniids strengthen the jelly ECM acting as a resilient structure against mechanical injuries, for example, coastal storms, predation or infauna colonization events, and also diseases. In the case of microbial infection, Maldonado et al. (2010) reported secretion of collagen barriers as defensive mechanism in *Ircinia* spp.

4.4 | Fibrous skeleton and fiber morphogenesis

The fibrous endoskeleton extended in the entire body of *I. retidermata* is complex and composed by collagen in a fibrous irregularly reticulate

network of primary fibers rich of incorporated exogenous materials, connected by secondary fibers free of exogenous material.

The consistent presence of an axial core containing varying amounts of sand grains and other exogenous material strongly indicates that mature primary fibers of *I. retidermata* are strengthened by these particles. This trait differs from *S. spinosulus*, which bears only few and scattered spicules embedded in collagenic primary fibers (Stocchino et al., 2021).

Each mature primary fiber of *I. retidermata* displays irregularly alternating linear cylindrical and laminar plated tracts along its length. Concentric laminar growth lines in the bark alternating with layers of amorphous matrix are shared with other Keratosa (Bergquist et al., 1998).

As for the presence of cells within the fiber pith, our data could match those of Vacelet (1971) who hypothesized the accidental inclusion of spongocytes during pith morphogenesis. Moreover, in *I. retidermata* the presence of collagenic material only in the ECM outside spongocytes (Masson and Azan) agrees with data provided by Vacelet (1971) on *Aplysina* spp. (as *Verongia* spp.).

About the detection of acidic glycans in the pith of cored fibers (blue-turquoise with Alcian blue), this could be due to residual ECM around inclusions during fibrogenesis.

The irregularly laminated inner pith is likely due to the fact that during early secretion phases of spongocytes, collagenic material accumulates irregularly around the included material, because the bearing axis of the included material does not have a regular shape.

In *I. retidermata* the fibers morphogenetic process seems to occur exclusively at ectosomal and outer endosome level by secretion of fibers *ex novo*. We suggest the following growth phases of *I. retidermata* fibers, which occur by sequential steps in the morphogenetic active zones. (1) A key process of fiber formation is the preliminary active incorporation and selection of detritus particles and their grouping in ectosomal areas that will drive morphogenesis using grains as condensation nucleus to produce the fiber axis. During incorporation, each grain appears surrounded by fibrillar/amorphous collagen; (2) spongocytes progressively grouped around detritus grains and secrete fibrillar/amorphous collagen to form the fibers pith, which gradually increase in thickness for concentric apposition of new layers at its surface; (3) these layers thicken and undergo collagenic material maturation as proto-spongin; (4) mature fibers are devoid of surrounding spongocytes. The destiny of these cells after their secretory activity is still unknown, although it has been hypothesized that would either restore their previous role in ECM or degenerate (see Vacelet, 1971 and references therein).

The morphogenetic processes of the fibrous complex layout in *I. retidermata*, driven by specialized cells as secretion of the fiber innermost part (pith) and consequent bark construction/assembling from the inside to the outside of the fiber, matches fibers morphogenesis reported for other Keratosa species (Bergquist, 1978; Bergquist et al., 1998; De Cook & Bergquist, 1998; Gaino, 2011; Minchin, 1900; Schulze, 1878a, 1878b, 1879a, 1879b; Simpson, 1984; Teragawa, 1986a, 1986b; Vacelet, 1971; von Lendenfeld, 1889). Fiber morphogenesis diverges in depth when comparing *I. retidermata* versus *S. spinosulus* as revealed by SEM and LM. Indeed, fiber formation occurs in *S. spinosulus* by means of the inward deposition of successive layers. Moreover, the main fibrous skeleton of *I. retidermata* is characterized by the absence of the active morphogenetic nodes within the mature fibers of *S. spinosulus* (Stocchino et al., 2021, Figure 9).

4.5 | Collagenic ectosomal complex architecture

The ectosome of *I. retidermata* has probably multiple functions. The ectosomal collagenic layout is polymorphic and assembled in a hierarchical architecture made of associated filamentous networks, parallel/radial distal fibers, and fibrillar networks.

This organic skeleton provides mechanical support for the entire body. This is particularly true for the outer subdermal areas with large canals/cavities filled of water, thus contributing, in cooperation with inhalant apertures/porocytes, to modulate the water inflow and pressure. In addition, collagenic filamentous honeycombed meshes at the body surface and their fine trellis-like network contribute to the modulation and selection of the amount and content of exogenous material in the inhaled water.

Ectosome and outer endosome districts are a germinative area where fibrogenesis occurs (Figure 13). The production of new fibers and secretion of new ECM between mature fibers determine the enlargement of body surface, with consequent morphogenesis of the underlying choanosomal district, drives the radial sponge growth. These morphogenetic processes may be related to the continuous morphogenesis and phenotypic plasticity typical of Porifera (Gaino et al., 1995).

The ectosome of *I. retidermata* probably functions in sponge-sediment relationship by trapping, incorporating, and selection of the material available in the water column. Different parts of *I. retidermata* body accumulate and use detritus particle in different ways at the level of ectosomal structures and fibers layout by recycling the reinforcing grains as reported for other species (e.g., Bavestrello et al., 1996, 1998; Schönberg, 2016; Teragawa, 1986a, 1986b). In *I.O retidermata*, fine grains are used to construct the sandy surface of ectosomal layer, while coarser grains form the axis of fibers. From an energetic point of view such mineral grain recycling from the water column may save energy as compared with the complex processes of spicule construction. From a mechanical point of view, collagenic structure strengthening by exogenous material inclusion may have been the evolutionary pressure that drove the successful morpho-anatomical evolution in Irciniidae and other families of Keratosa. Active sediment uptake and its recycling by incorporation in collagenic structures seem to be a successful strategy probably due to the natural affinity among surfaces of sponge collagenic material and mineral particles. This is in agreement with Krasko et al. (2000), Müller et al. (2004), and Pozzolini et al. (2012) reporting that silicate has a morphogenetic activity by increasing gene expression of collagen, although this may also be induced by calcium carbonate grains.

The data presented here on the morphogenetic process match those of other soft sponges of the order Dictyoceratida, that is, fibers

are synthesized by discrete groups of specialized cells that also drive their assembling. In *I. retidermata* the secretion of the innermost part of the fibers start around grains by conjoint action of spongocytes with a construction occurring by apposition from inside to outside as first shown by Schulze (1878a, 1878b, 1879a, 1879b) and von Lendenfeld (1889) and as subsequently reported by several authors for various taxa (Bergquist, 1978; Bergquist et al., 1998; De Cook & Bergquist, 1998; Gaino, 2011; Minchin, 1900; Simpson, 1984; Teragawa, 1986a, 1986b; Vacelet, 1971).

5 | CONCLUSIONS

The prototype of connective system, here characterized in a model basal metazoan is almost exclusively based on collagenic networks widely diversified. The topographic distribution, spatial layout, micro-traits, and/or morphogenesis of collagenic structures of *Ircinia retidermata* are focused. Outer body districts are the active fibrogenetic areas where the exogenous inorganic material plays the role of key condensation nucleus for the ensuing morphogenesis of ECM and fibrous skeleton. Further, the collagenic material is diversified in the different structures (e.g., filament versus fibers) and in different parts of the same structure (e.g., filament). These materials confer plasticity to the organization of sponge connective system and support key evolutionary novelties at the level of (a) aquiferous system devoted to water circulation, (b) cell clusters competent for nutrient transfer, (c) filamentous skeletal system and (d) fibrous skeletal system.

In synthesis, our bulk of data on architectural diversity of connective system of *I. retidermata* confirms that sponges are a key model phylum to understand the origin of the ECM complexity and animal multicellularity. This could be a cue to explain both the evolutionary novelties displayed by irciniids and functional significance of their adaptive anatomical traits. At the same time, our data support both systematics and phylogenetic analyses together with marine collagen applied research. Indeed, collagenic sponge material was proved to enhance for example drug delivery (Langasco et al., 2017; Rahman, 2021; Swatschek et al., 2002) and to promote bone mineralization (Granito et al., 2017; Green et al., 2003; Kim et al., 2009). Soft body sponges are confirmed as versatile and multifaceted source of bioinspired materials.

ACKNOWLEDGMENTS

We thank Nicola Rassu, Giuseppe Agliega, and Antonello Floris (Università di Sassari) for their kind cooperation. We are grateful to Club Nautico Capo Caccia and its staff for the kind logistic support at the Tramariglio marina.

AUTHOR CONTRIBUTIONS

Renata Manconi: Conceptualization (lead); data curation (lead); investigation (lead); methodology (lead); project administration (lead); resources (lead); supervision (lead); validation (lead); visualization (lead); writing – original draft (lead); writing – review and editing (lead). **Tiziana Cubeddu:** Conceptualization (lead); data curation (lead); investigation (lead); methodology (lead); resources (lead); supervision (lead); validation (lead); visualization (lead); writing – original draft (lead); writing – review and editing (lead). **Roberto Pronzato:** Data curation (lead); investigation (equal); methodology (equal); resources (lead); supervision (lead); validation (lead); visualization (lead); writing – original draft (lead); writing – review and editing (lead). **Marina Sanna:** Data curation (supporting). **Gabriele Nieddu:** Data curation (supporting); writing – review and editing (supporting). **Elda Gaino:** Formal analysis (equal); validation (equal); writing – review and editing (lead). **Giacinta A. Stocchino:** Conceptualization (lead); data curation (lead); investigation (lead); methodology (lead); resources (lead); supervision (lead); validation (lead); visualization (lead); writing – original draft (lead); writing – review and editing (lead).

CONFLICT OF INTERESTS

The authors declare that the research was conducted in the absence of any commercial or financial relationships that could be construed as a potential conflict of interest.

PEER REVIEW

The peer review history for this article is available at https://publons.com/publon/10.1002/jmor.21460.

DATA AVAILABILITY STATEMENT

Data available on request from the authors.

ORCID

Renata Manconi https://orcid.org/0000-0002-7619-8493

REFERENCES

Aouacheria, A., Geourjon, C., Aghajari, N., Navratil, V., Deléage, G., Lethias, C., & Exposito, J. Y. (2006). Insights into early extracellular matrix evolution: Spongin short chain collagen-related proteins are homologous to basement membrane type IV collagens and form a novel family widely distributed in invertebrates. *Molecular Biology and Evolution*, *23*, 2288–2302.

Bavestrello, G., Arillo, A., Calcinai, B., Cerrano, C., Lanza, S., Sara', M., Cattaneo-Vietti, R., & Gaino, E. (1998). Siliceous particles incorporation in *Chondrosia reniformis* (Porifera, Demospongiae). *The Italian Journal of Zoology*, *65*(4), 343–348.

Bavestrello, G., Cerrano, C., Cattaneo-Vietti, R., Sarà, M., Calabria, F., & Cortesogno, L. (1996). Selective incorporation of foreign material in *Chondrosia reniformis* (Porifera, Demospongiae). *The Italian Journal of Zoology*, *63*(3), 215–220.

Bergquist, P. R. (1978). *Sponges*. Hutchinson University Library, London & University of California Press.

Bergquist, P. R. (1980). A revision of the supraspecific classification of the orders Dictyoceratida, Dendroceratida, and Verongida (class Demospongiae). *New Zealand Journal of Zoology*, *7*(4), 443–503. https://doi.org/10.1080/03014223.1980.11760680

Bergquist, P. R., Walsh, D., & Gray, R. D. (1998). Relationships within and between the orders of Demospongiae that lack a mineral skeleton. In Y. Watanabe & N. Fusetani (Eds.), *Sponge science: Multidisciplinary perspectives* (pp. 31–40). Tokyo, Berlin, Heidelberg, New York: Springer-Verlag.

Boury-Esnault, N., & Rützler, K. (1997). *Thesaurus of sponge morphology. Smithsonian contributions to zoology 596*. Washington D.C.: Smithsonian Institution Press.

Brien, P., Lévi, C., Sarà, M., Tuzet, O., & Vacelet, J. (1973). Spongiaires. In P. P. Grassé (Ed.), *Traité de Zoologie. Anatomie, Systématique, Biologie. Spongiaires* (Vol. 3). Masson et C.ie Editeurs.

Carter, H. J. (1880). VIII.—Report on specimens dredged up from the Gulf of Manaar and presented to the Liverpool Free Museum by Capt. WH Cawne Warren. *Journal of Natural History*, *6*(31), 35–61.

Cowden, R. R. (1970). Connective tissue in six marine sponges: A histological and histochemical study. *Zeitschrift für Mikroskopisch-Anatomische Forschung*, *82*(4), 557–569.

Cowden, R. R., & Harrison, F. W. (1976). Cytochemical studies of connective tissues in sponges. In F. W. Harrison & R. R. Cowden (Eds.), *Aspects of sponge biology* (pp. 69–82). Academic Press. https://doi.org/10.1016/B978-0-12-327950-7.50011-7

Da Hora, J., Cavalcanti, F. F., & Lanna, E. (2018). Anatomy and ultrastructure of the tropical sponge *Cladocroce caelum* (Haplosclerida, Demospongiae). *Journal of Morphology*, *279*(12), 1872–1886.

de Caralt, S., Agell, G., & Uriz, M. J. (2003). Long-term culture of sponge explants: Conditions enhancing survival and growth, and assessment of bioactivity. *Biomolecular Engineering*, *20*(4–6), 339–347.

De Cook, S. C., & Bergquist, P. R. (1998). Revision of the genus *Psammocinia* (Porifera: Demospongiae: Dictyoceratida), with six new species from New Zealand. *New Zealand Journal of Marine and Freshwater Research*, *32*, 399–426. https://doi.org/10.1080/00288330.1998.9516834

De Cook, S. C., & Bergquist, P. R. (2002). Order Dictyoceratida Minchin, 1900. In J. N. A. Hooper, R. W. M. van Soest, & P. Willenz (Eds.), *Systema Porifera: A guide to the classification of sponges* (pp. 1021–1066). New York, Boston, Dordrecht, London, Moscow: Kluwer Academic / Plenum Publisher.

Eherlich, H., Wysokowski, M., Zoltowska-Aksamitowska, S., Petrenko, I., & Jesionowski, T. (2018). Collagens of poriferan origin. *Marine Drugs*, *16*, 9. https://doi.org/10.3390/md16030079

Ereskovsky, A., & Lavrov, A. (2021). Porifera. In E. E. B. LaDouceur (Ed.), *Invertebrate histology* (pp. 19–54). Hoboken, New Jersey: Wiley-Blackwell.

Erpenbeck, D., Galitz, A., Ekins, M., De Cook, S. C., van Soest, R. W. M., Hooper, J. N., & Wörheide, G. (2020). Soft sponges with tricky tree: On the phylogeny of dictyoceratid sponges. *Journal of Zoological Systematics and Evolutionary Research*, *58*(1), 27–40. https://doi.org/10.1111/jzs.12351

Erpenbeck, D., Sutcliffe, P., De Cook, S. C., Dietzel, A., Maldonado, M., Van Soest, R. W. M., Hooper, J. N. A., & Wörheide, G. (2012). Horny sponges and their affairs: On the phylogenetic relationships of keratose sponges. *Molecular Phylogenetics and Evolution*, *63*(3), 809–816. https://doi.org/10.1016/j.ympev.2012.02.024

European Commission. (2012). *Blue Growth: Opportunities for Marine and Maritime Sustainable Growth: communication from the Commission to the European Parliament, the Council, the European Economic and Social Committee and the Committee of the Regions*. Luxemburg: Publications Office of the European Union. https://data.europa.eu/doi/10.2771/43949

Exposito, J. Y., Cluzel, C., Garrone, R., & Lethias, C. (2002). Evolution of collagens. *The Anatomical Record: An Official Publication of the American Association of Anatomists*, *268*(3), 302–316.

Exposito, J. Y., Le Guellec, D., Lu, Q., & Garrone, R. (1991). Short chain collagens in sponges are encoded by a family of closely related genes. *International Journal of Biological Chemistry*, *266*, 21923–21928.

Exposito, J. Y., Ouazana, R., & Garrone, R. (1990). Cloning and sequencing of a Porifera partial CDNA coding for a short-chain collagen. *European Journal of Biochemistry*, *190*(2), 401–406.

Gaino, E. (2011). Overview of Porifera. In M. Pansini, R. Manconi, & R. Pronzato (Eds.), *Fauna d'Italia Vol. 46. Porifera I. Calcarea, Demospongiae (partim), Hexactinellida, Homoscleromorpha* (pp. 1–53). Bologna: Calderini.

Gaino, E., Manconi, R., & Pronzato, R. (1995). Organizational plasticity as a successful conservative tactics in sponges. *Animal Biology*, *4*, 31–43.

Garrone, R. (1978). *Phylogenesis of connective tissue. Morphological aspects and biosynthesis of sponge intercellular matrix*. Basel: S. Karger.

Garrone, R. (1985). The collagen of the Porifera. In A. Bairati & R. Garrone (Eds.), *Biology of invertebrate and lower vertebrate collagens* (pp. 157–175). Boston, MA: Springer. https://doi.org/10.1007/978-1-4684-7636-1_12

Garrone, R. (1998). Evolution of metazoan collagens. *Progress in Molecular and Subcellular Biology*, *21*, 191–193.

Garrone, R. (1999). Collagen, a common thread in extracellular matrix evolution. *Proceedings of the Indian Academy of Sciences-Chemical Sciences*, Springer India, *111*(1), 51–56.

Garrone, R., Huc, A., & Junqua, S. (1975). Fine structure and physiochemical studies on the collagen of the marine sponge *Chondrosia reniformis* Nardo. *Journal of Ultrastructure Research*, *52*, 261–275.

Garrone, R., Vacelet, J., Pavans de Ceccatty, M., Junqua, S., Robert, L., & Huc, A. (1973). Une formation collagène particulière: les filaments des éponges cornées *Ircinia*. Étude ultrastructurale, physico-chimique et biochimique. *Journal of Microscopy*, *17*, 241–260.

Gökalp, M., Mes, D., Nederlof, M., Zhao, H., Merijn de Goeij, J., & Osinga, R. (2021). The potential roles of sponges in integrated mariculture. *Reviews in Aquaculture*, *13*(3), 1159–1171. https://doi.org/10.1111/raq.12516

Gökalp, M., Wijgerde, T., Murk, A., & Osinga, R. (2021). Design for large-scale maricultures of the Mediterranean demosponge *Chondrosia reniformis* Nardo, 1847 for collagen production. *Aquaculture*, *548*, 737702.

Granito, R. N., Custodio, M. R., & Renno, A. C. M. (2017). Natural marine sponges for bone tissue engineering: The state of art and future perspectives. *Journal of Biomedical Materials Research Part B Applied Biomaterials*, *105*(6), 1717–1727. https://doi.org/10.1002/jbm.b.33706

Gray, J. E. (1867). Notes on the arrangement of sponges, with the descriptions of some new genera. *Proceedings of the Zoological Society of London*, *1867*(2), 492–558.

Green, D., Howard, D., Yang, X., Kelly, M., & Oreffo, R. O. C. (2003). Natural marine sponge fibre skeleton: A biomimetic scaffold for human osteoprogenitor cell attachment, growth and differentiation. *Tissue Engineering*, *9*(6), 1159–1166.

Gross, J., Sokal, Z., & Rougvie, M. (1956). Structural and chemical studies on the connective tissue of marine sponges. *Journal of Histochemistry and Cytochemistry*, *4*(3), 227–246. https://doi.org/10.1177/4.3.227

Heinemann, S., Ehrlich, H., Douglas, T., Heinemann, C., Worch, H., Schatton, W., & Hanke, T. (2007). Ultrastructural studies on the collagen of the marine sponge *Chondrosia reniformis* Nardo. *Biomacromolecules*, *8*(11), 3452–3457.

Junqua, S., Robert, L., Garrone, R., Pavans de Ceccatty, M., & Vacelet, J. (1974). Biochemical and morphological studies on collagens of horny sponges. *Ircinia* filaments compared to spongines. *Connective Tissue Research*, *2*, 193–203. https://doi.org/10.3109/03008207409152244

Kenneth, M. T., & Rützler, K. (1968). Lepidocrocite iron mineralization in Keratose sponge granules. Lepidocrocite iron mineralization in Keratose sponge granules. *Science*, *162*(3850), 268–269. https://doi.org/10.1126/science.162.3850.268

Kim, M. M., Mendis, E., Rajapakse, N., Lee, S. H., & Kim, S. K. (2009). Effect of spongin derived from *Hymeniacidon sinapium* on bone mineralization. *Journal of Biomedical Materials Research Part B: Applied Biomaterials*, *90*(2), 540–546.

Krasko, A., Lorenz, B., Batel, R., Schröder, H. C., Müller, I. M., & Müller, W. E. (2000). Expression of silicatein and collagen genes in the marine sponge *Suberites domuncula* is controlled by silicate and myotrophin. *European Journal of Biochemistry*, *267*(15), 4878–4887.

Langasco, R., Cadeddu, B., Formato, M., Lepedda, A. J., Cossu, M., Giunchedi, P., Pronzato, R., Rassu, G., Manconi, R., & Gavini, E. (2017). Natural collagenic skeleton of marine sponges in pharmaceutics:

Innovative biomaterial for topical drug delivery. *Materials Science and Engineering C*, *70*, 710–720.

Ledda, F. D., Pronzato, R., & Manconi, R. (2014). Mariculture for bacterial and organic waste removal: A field study of sponge filtering activity in experimental farming. *Aquaculture Research*, *45*(8), 1389–1401.

Leys, S. P., & Reiswig, H. M. (1998). Transport pathways in the neotropical sponge *Aplysina*. *The Biological Bulletin*, *195*(1), 30–42.

Lim, Y. S., Ok, Y. J., Hwang, S. Y., Kwak, J. Y., & Yoon, S. (2019). Marine collagen as a promising biomaterial for biomedical applications. *Marine Drugs*, *17*(8), 467.

Maldonado, M., Sánchez-Tocino, L., & Navarro, C. (2010). Recurrent disease outbreaks in corneous demosponges of the genus *Ircinia*: Epidemic incidence and defense mechanisms. *Marine Biology*, *157*(7), 1577–1590. https://doi.org/10.1007/s00227-010-1431-7

Manconi, R., Cadeddu, B., Ledda, F. D., & Pronzato, R. (2013). An overview of the Mediterranean cave-dwelling horny sponges (Porifera, Demospongiae). *ZooKeys*, *28*, 1–68. https://doi.org/10.3897/zookeys.281.4171

Manconi, R., Padiglia, A., Cubeddu, T., & Pronzato, R. (2019). Long-term sponge stranding along the shores of Sardinia Island (Western Mediterranean Sea). *Marine Ecology*, *40*(6), e12567. https://doi.org/10.1111/maec.12567

Manconi, R., Padiglia, A., Padedda, B. M., & Pronzato, R. (2020). Invasive green algae in a western Mediterranean marine protected area: Interaction of photophilous sponges with *Caulerpa cylindracea*. *Journal of the Marine Biological Association of the United Kingdom*, *100*, 361–373. https://doi.org/10.1017/S0025315420000193

Martins, E., Rocha, M. S., Silva, T. H., & Reis, R. L. (2019). Chapter 2. Remarkable body architecture of marine sponges as biomimetic structure for application in tissue engineering. In A. H. Choi & B. Ben-Nissan (Eds.), *Marine-derived biomaterials for tissue engineering applications* (pp. 27–50). Springer Series in Biomaterials Science and Engineering, Singapore: Springer Nature. https://doi.org/10.1007/978-981-13-8855-2_2

Minchin, E. A. (1900). Chapter III. Sponges. In E. R. Lankester (Ed.), *A treatise on zoology*. *Part II. The Porifera and Coelenterata* (Vol. 2, pp. 1–178). Adam & Charles Black.

Müller, W. E., Wiens, M., Adell, T., Gamulin, V., Schröder, H. C., & Müller, I. M. (2004). Bauplan of Urmetazoa: Basis for genetic complexity of Metazoa. *International Review of Cytology*, *235*, 53–92.

Müller, W. E. G. (1997). Origin of metazoan adhesion molecules and adhesion receptors as deduced from cDNA analyses in the marine sponge *Geodia cydonium*: A review. *Cell and Tissue Research*, *289*, 383–395.

Müller, W. E. G. (1998a). In W. E. G. Müller, *Molecular evolution: Evidence for monophyly of Metazoa* (p. 189). Progress in Molecular and Subcellular Biology, Berlin, Heidelberg: Springer-Verlag. https://doi.org/10.1007/978-3-642-48745-3

Müller, W. E. G. (1998b). In W. E. G. Müller, *Molecular evolution: Towards the origin of Metazoa* (p. 185). Progress in Molecular and Subcellular Biology, Berlin, Heidelberg: Springer-Verlag. https://doi.org/10.1007/978-3-642-72236-3

Murray, P. M., Moane, S., Collins, C., Beletskaya, T., Thomas, O. P., Duarte, A. W. F., Nobre, F. S., Owoyemi, I. O., Pagnocca, F. C., Sette, L. D., McHugh, E., Causse, E., Pérez-López, P., Feijoo, G., Moreira, M. T., Rubiolo, J., Leirós, M., Botana, L. M., Pinteus, S., … Walsh, D. J. (2013). Sustainable production of biologically active molecules of marine based origin. *New Biotechnology*, *30*, 839–850.

Nicklas, M., Schatton, W., Heinemann, S., Hanke, T., & Kreuter, J. (2009a). Preparation and characterization of marine sponge collagen nanoparticles and employment for the transdermal delivery of 17β-estradiol-hemihydrate. *Drug Development and Industrial Pharmacy*, *35*(9), 1035–1042. https://doi.org/10.1080/03639040902755213

Nicklas, M., Schatton, W., Heinemann, S., Hanke, T., & Kreuter, J. (2009b). Enteric coating derived from marine sponge collagen. *Drug Development and Industrial Pharmacy*, *35*(11), 1384–1388. https://doi.org/10.3109/03639040902939239

Orel, B., Giovine, M., & Ilan, M. (2021). On the path to thermo-stable collagen: Culturing the versatile sponge *Chondrosia reniformis*. *Marine Drugs*, *19*, *669*. https://doi.org/10.3390/md19120669

Padiglia, A., Ledda, F. D., Padedda, B. M., Pronzato, R., & Manconi, R. (2018). Long-term experimental *in situ* farming of *Crambe crambe* (Demospongiae: Poecilosclerida). *PeerJ*, *6*, e4964. https://doi.org/10.7717/peerj.4964

Pallela, R., Bojja, S., & Janapala, V. R. (2011). Biochemical and biophysical characterization of collagens of marine sponge, *Ircinia fusca* (Porifera: Demospongiae: Irciniidae). *International Journal of Biological Macromolecules*, *49*(1), 85–92.

Pallela, R., Venkatesan, J., Janapala, V. R., & Kim, S. K. (2012). Biophysicochemical evaluation of chitosan-hydroxyapatite-marine sponge collagen composite for bone tissue engineering. *Journal of Biomedical Materials Research. Part A*, *100*, 486–495.

Perez-Lopez, P., Ledda, F. D., Bisio, A., Feijoo, G., Perino, E., Pronzato, R., Manconi, R., & Moreira, M. T. (2017). Life cycle assessment of *in situ* mariculture in the Mediterranean Sea for the production of bioactive compounds from the sponge *Sarcotragus spinosulus*. *Journal of Cleaner Production*, *142*, 4356–4368. https://doi.org/10.1016/j.jclepro.2016.11.137

Pozzolini, M., Bruzzone, F., Berilli, V., Mussino, F., Cerrano, C., Benatti, U., & Giovine, M. (2012). Molecular characterization of a Nonfibrillar collagen from the marine sponge *Chondrosia reniformis* Nardo 1847 and positive effects of soluble silicates on its expression. *Marine Biotechnology*, *14*(3), 281–293.

Pozzolini, M., Scarfi, S., & Giovine, M. (2020). Chapter 39. Marine collagen and its Biotechnological Applications. In S. K. Kim (Ed.), *Encyclopedia of Marine Biotechnology: Five Volume Set* (Vol. 2, 1st ed., pp. 1007–1030). Hoboken, New Jersey: John Wiley & Sons Ltd. https://doi.org/10.1002/9781119143802.ch39

Pronzato, R. (1999). Sponge-fishing, disease and farming in the Mediterranean Sea. *Aquatic Conservation: Marine and Freshwater Ecosystems*, *9*, 485–493.

Pronzato, R., Bavestrello, G., Cerrano, C., Magnino, G., Manconi, R., Pantelis, J., Sarà, A., & Sidri, M. (1999). Sponge farming in the Mediterranean Sea: New perspectives. *Memories of the Queensland Museum*, *44*, 485–491.

Pronzato, R., & Manconi, R. (2011). Class Demospongiae. Order Dendroceratida, Dictyoceratida, Verongida, Halisarcida. In M. Pansini, R. Manconi, & R. Pronzato (Eds.), *Porifera I. Calcarea*, *Demospongiae (partim)*, *Hexactinellida*, *Homoscleromorpha*. *Fauna d'Italia*, (Vol. 46, pp. 245–340). Bologna: Calderini-Il Sole 24 Ore.

Pulitzer-Finali, G., & Pronzato, R. (1980). The Keratosa in a collection of Mediterranean sponges mainly from the Italian coasts. *Annali del Museo Civico di Storia Naturale "Giacomo Doria"*, *83*, 123–158.

Rahman, A. (Ed.). (2021). *Marine Skeletal Biopolymers and Proteins*, *and their Biomedical Application*. (p. 220). Basel: Marine Drugs, MDPI. https://doi.org/10.3390/books978-3-0365-2133-6

Schönberg, C. H. L. (2016). Happy relationships between marine sponges and sediments–a review and some observations from Australia. *Journal of the Marine Biological Association of the United Kingdom*, *96*(2), 493–514. https://doi.org/10.1017/S0025315415001411

Schröder, H. C., Krasko, A., Batel, R., Skorokhod, A., Pahler, S., Kruse, M., Müller, I. M., & Müller, W. E. G. (2000). Stimulation of protein (collagen) synthesis in sponge cells by a cardiac myotrophin-related molecule from *Suberites domuncula*. *The FASEB Journal*, *14*, 2022–2031.

Schulze, F. E. (1878a). Untersuchungen über den Bau und die Entwicklung der Spongien. Vierte Mittheilung. Die Familie der Aplysinidae. *Zeitschrift für wissenschaftliche Zoologie*, *30*, 379–420.

Schulze, F. E. (1878b). Untersuchungen über den Bau und die Entwicklung der Spongien. Sechste mittheilung. Die gattung *Spongelia*. *Zeitschrift für wissenschaftliche Zoologie*, *32*, 117–157.

Schulze, F. E. (1879a). Untersuchungen über den Bau und die Entwicklung der Spongien. Siebente Mittheilung. Die Familie der Spongidae. *Zeitschrift für wissenschaftliche Zoologie*, *32*, 593–660.

Schulze, F. E. (1879b). Untersuchungen über den Bau und die Entwicklung der Spongien. Achte Mittheilung. Die Gattung *Hircinia* Nardo und *Oligoceras* ng. *Zeitschrift für wissenschaftliche Zoologie*, *33*, 1–38.

Silva, T. H., Moreira-Silva, J., Marques, A. L. P., Domingues, A., Bayon, Y., & Reis, R. L. (2014). Marine origin collagens and its potential applications. *Marine Drugs*, *12*(12), 5881–5901.

Sim, C. J., & Lee, K. J. (1999). Relationship of sand and fibre in the horny sponge *Psammocinia*. *Memoirs of the Queensland Museum*, *44*, 551–557.

Sim, C. J., & Lee, K. J. (2002a). Two new psammocinian sponges (Dictyoceratida: Irciniidae) from Korea. *Korean Journal of Biological Sciences*, *6*, 53–57. https://doi.org/10.1080/12265071.2002.9647633

Sim, C. J., & Lee, K. J. (2002b). A new species in the family Irciniidae (Demospongiae: Dictyoceratida) from Korea. *Korean Journal of Biological Sciences*, *6*, 283–285. https://doi.org/10.1080/12265071.2002.9647664

Simpson, T. L. (1984). *The cell biology of sponges*. Springer-Verlag. https://doi.org/10.1007/978-1-4612-5214-6

Stocchino, G. A., Cubeddu, T., Pronzato, R., Sanna, M. A., & Manconi, R. (2021). Sponges architecture by colour: New insights into the fibres morphogenesis, skeletal spatial layout and morpho-anatomical traits of a marine horny sponge species (Porifera). *European Zoological Journal*, *88*(1), 237–253. https://doi.org/10.1080/24750263.2020.1862316

Swatschek, D., Schatton, W., Müller, W. E., & Kreuter, J. (2002). Microparticles derived from marine sponge collagen (SCMPs): Preparation, characterization and suitability for dermal delivery of all-trans retinol. *European Journal of Pharmaceutics and Biopharmaceutics*, *54*(2), 125–133.

Teragawa, C. K. (1986a). Sponge dermal membrane morphology: Histology of cell-mediated particle transport during skeletal growth. *Journal of Morphology*, *190*, 335–347. https://doi.org/10.1002/jmor.1051900310

Teragawa, C. K. (1986b). Particle transport and incorporation during skeleton formation in a keratose sponge: *Dysidea etheria*. *Biological Bullettin*, *170*, 321–334. https://doi.org/10.2307/1541812

Ternon, E., Perino, E., Manconi, R., Pronzato, R., & Thomas, O. P. (2017). How environmental factors affect the production of guanidine alkaloids by the Mediterranean sponge *Crambe crambe*. *Marine Drugs*, *15*, 181.

Tziveleka, L. A., Ioannou, E., Tsiourvas, D., Berillis, P., Foufa, E., & Roussis, V. (2017). Collagen from the marine sponges *Axinella cannabina* and *Suberites carnosus*: Isolation and morphological, biochemical, and biophysical characterization. *Marine Drugs*, *15*(6), 152. https://doi.org/10.3390/md15060152

Vacelet, J. (1959). Répartition générale des éponges et systématique des épongés cornées de la région de Marseille et de quelques stations méditerranéennes. *Recueil des Travaux de la Station Marine d'Endoume*, *16*(26), 39–101.

Vacelet, J. (1971). Ultrastructure et formation des fibres de spongine d'Eponges Cornees *Verongia*. *Journal of Microscopy*, *10*, 13–32.

Vacelet, J., Verdenal, B., & Perinet, G. (1988). The iron mineralization of *Spongia officinalis* L. (Porifera, Dictyoceratida) and its relationships with the collagen skeleton. *Biology of the Cell*, *62*, 189–198.

von Lendenfeld, R. (1889). *A monograph of the horny sponges*. London: Trübner and Co.

Wang, W., Itoh, S., Aizawa, T., Okawa, A., Sakai, K., Ohkuma, T., & Demura, M. (2010). Development of an injectable chitosan/marine collagen composite gel. *Biomedical Materials*, *5*, 065009.

Wanick, R., Mermelstein, C., Andrade, I. R., Santelli, R. E., Paranhos, R. P., & Coutinho, C. C. (2017). Distinct histomorphology for growth arrest and digitate outgrowth in cultivated *Haliclona* sp. (Porifera: Demospongiae). *Journal of Morphology*, *278*(12), 1682–1688.

Wanick, R. C., Vieira, R. P., Santelli, R. E., Da, R. P., Paranhos, R. P., & Coutinho, C. C. (2015). Screening for cultivable species of marine sponges (Porifera) in an ecologically inspired ex situ system. *Journal of FisheriesSciences.com*, *9*, 5–11.

SUPPORTING INFORMATION

Additional supporting information may be found in the online version of the article at the publisher's website.

How to cite this article: Manconi, R., Cubeddu, T., Pronzato, R., Sanna, M. A., Nieddu, G., Gaino, E., & Stocchino, G. A. (2022). Collagenic architecture and morphotraits in a marine basal metazoan as a model for bioinspired applied research. *Journal of Morphology*, *283*(5), 585–604. https://doi.org/10.1002/jmor.21460